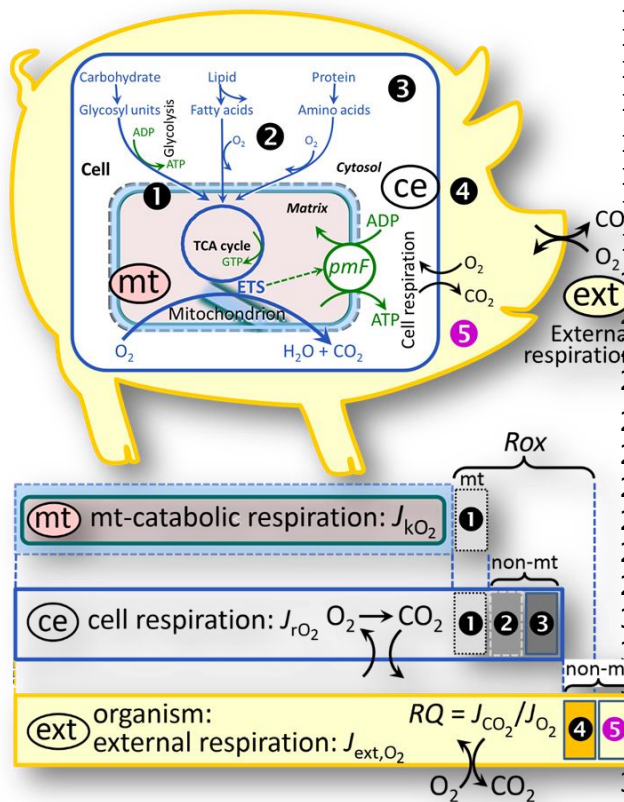


Mitochondrial physiology

2. Respiratory states and rates

MitoEAGLE Task Group*

Living Communication: extended resource of **Mitochondrial respiratory states and rates. Nat Metab** (Gnaiger *et al*, in review); from Gnaiger *et al* (2020) Bioenerg Commun 2020.1.



Overview

Internal and external respiration

(mt) **Mitochondrial catabolic respiration**, J_{kO_2} , is the O_2 consumption in the oxidation of fuel substrates (electron donors) and reduction of O_2 catalysed by the electron transfer system, ETS, which drives the protonmotive force, pmF . J_{kO_2} excludes mitochondrial residual oxygen consumption, mt-Rox (1).

(ce) **Cell respiration** or internal cellular O_2 consumption, J_{rO_2} , takes into account all chemical reactions, r , that consume O_2 in the cells. Catabolic cell respiration is the O_2 consumption associated with catabolic pathways in the cell, including (mt) mitochondrial catabolism; mt-Rox (1); non-mt O_2 consumption by catabolic reactions, particularly peroxisomal oxidases and microsomal cytochrome P450 systems (2); and non-mt Rox by reactions unrelated to catabolism (3).

(ext) **External respiration** balances internal respiration at steady-state,

including extracellular Rox (4) and aerobic respiration by the microbiome (5).

O_2 is transported from the environment across the respiratory cascade, *i.e.*, circulation between tissues and diffusion across cell membranes, to the intracellular compartment. The respiratory quotient, RQ , is the molar CO_2/O_2 exchange ratio; when combined with the respiratory nitrogen quotient, N/O_2 (mol N given off per mol O_2 consumed), the RQ reflects the proportion of carbohydrate, lipid and protein utilized in cell respiration during aerobically balanced steady-states. Bicarbonate and CO_2 are transported in reverse to the extracellular milieu and the organismic environment. Hemoglobin provides the molecular paradigm for the combination of O_2 and CO_2 exchange, as do lungs, gills, the skin and other surfaces on the morphological level.

Respiratory states are defined in Table 1. Rates are illustrated in Figure 5. Consult Table 8 for a list of terms and symbols.

Updates:

https://www.bioenergetics-communications.org/index.php/BEC2020.1_doi10.26124bec2020-0001.v1

Table and Figure numbers refer to Gnaiger *et al* (2020) Bioenerg Commun 2020.1.

Table of contents

56	Abstract – Executive summary
57	1. Part 2. States and rates
58	2. Coupling states and rates in mitochondrial preparations
59	2.1. Cellular and mitochondrial respiration
60	2.1.1. Aerobic and anaerobic catabolism and ATP turnover
61	2.1.2. Specification of biochemical dose
62	2.2. Mitochondrial preparations
63	2.3. Electron transfer pathways
64	2.4. Respiratory coupling control
65	2.4.1. Coupling
66	2.4.2. Phosphorylation, P_{\gg} , and P_{\gg}/O_2 ratio
67	2.4.3. Uncoupling
68	2.5. Coupling states and respiratory rates
69	2.5.1. LEAK-state
70	2.5.2. OXPHOS-state
71	2.5.3. Electron transfer-state
72	2.5.4. ROX state and R_{ox}
73	2.5.5. Quantitative relations
74	2.5.6. The steady-state
75	2.6. Classical terminology for isolated mitochondria
76	2.6.1. – 2.6.5. State 1 – State 5
77	2.7. Control and regulation
78	3. What is a rate? – Box 1: Metabolic flows and fluxes: vectoral, vectorial, and scalar
79	4. Normalization of rate per sample
80	4.1. Flow: per object
81	4.1.1. Number concentration
82	4.1.2. Flow per object
83	4.2. Size-specific flux: per sample size
84	4.2.1. Sample concentration
85	4.2.2. Size-specific flux
86	4.3. Marker-specific flux: per mitochondrial content
87	4.3.1. Mitochondrial concentration and mitochondrial markers
88	4.3.2. mt-Marker-specific flux
89	5. Normalization of rate per system
90	5.1. Flow: per chamber
91	5.2. Flux: per chamber volume
92	5.2.1. System-specific flux
93	5.2.2. Advancement per volume
94	6. Conversion of units
95	7. Conclusions – Box 2: Recommendations for studies with mitochondrial preparations
96	References
97	Authors (MitoEAGLE Task Group) – Author contributions
98	Acknowledgements – Competing financial interests – Correspondence
99	

100 Abstract

101
102 **As the knowledge base and importance of mitochondrial physiology to evolution, health**
103 **and disease expands, the necessity for harmonizing the terminology concerning**
104 **mitochondrial respiratory states and rates has become increasingly apparent. The**
105 **chemiosmotic theory establishes the mechanism of energy transformation and coupling in**
106 **oxidative phosphorylation. The unifying concept of the protonmotive force provides the**
107 **framework for developing a consistent theoretical foundation of mitochondrial physiology**
108 **and bioenergetics. We follow guidelines of the International Union of Pure and Applied**
109 **Chemistry (IUPAC) on terminology in physical chemistry, extended by considerations of**
110 **open systems and thermodynamics of irreversible processes. The concept-driven**
111 **constructive terminology incorporates the meaning of each quantity and aligns concepts**

112 **and symbols with the nomenclature of classical bioenergetics. We endeavour to provide a**
113 **balanced view of mitochondrial respiratory control and a critical discussion on reporting**
114 **data of mitochondrial respiration in terms of metabolic flows and fluxes. Uniform**
115 **standards for evaluation of respiratory states and rates will ultimately contribute to**
116 **reproducibility between laboratories and thus support the development of databases of**
117 **mitochondrial respiratory function in species, tissues, and cells. Clarity of concept and**
118 **consistency of nomenclature facilitate effective transdisciplinary communication,**
119 **education, and ultimately further discovery.**

120
121 *Keywords:* Mitochondrial respiratory control, coupling control, mitochondrial preparations,
122 protonmotive force, uncoupling, oxidative phosphorylation: OXPHOS, efficiency, electron
123 transfer: ET, electron transfer system: ETS, proton leak, ion leak and slip compensatory state:
124 LEAK, residual oxygen consumption: ROX, State 2, State 3, State 4, normalization, flow, flux,
125 oxygen: O₂

127 **Executive summary**

128
129 In view of the broad implications for health care, mitochondrial researchers face an increasing
130 responsibility to disseminate their fundamental knowledge and novel discoveries to a wide range
131 of stakeholders and scientists beyond the group of specialists. This requires implementation of a
132 commonly accepted terminology within the discipline and standardization in the translational
133 context. Authors, reviewers, journal editors, and lecturers are challenged to collaborate with the
134 aim to harmonize the nomenclature in the growing field of mitochondrial physiology and
135 bioenergetics, from evolutionary biology and comparative physiology to mitochondrial medicine.
136 In the present communication we focus on the following concepts in mitochondrial physiology:

137
138 1. Aerobic respiration is the O₂ flux in catabolic reactions coupled to phosphorylation of ADP to
139 ATP, and O₂ flux in a variety of O₂ consuming reactions apart from oxidative phosphorylation
140 (OXPHOS). Coupling in OXPHOS is mediated by the translocation of protons across the
141 mitochondrial inner membrane (mtIM) through proton pumps generating or utilizing the
142 protonmotive force that is maintained between the mitochondrial matrix and intermembrane
143 compartment or outer mitochondrial space. Compartmental coupling depends on ion
144 translocation across a semipermeable membrane, which is defined as vectorial metabolism and
145 distinguishes OXPHOS from cytosolic fermentation as counterparts of cellular core energy
146 metabolism (**Overview**). Cell respiration is thus distinguished from fermentation: (1) Electron
147 acceptors are supplied by external respiration for the maintenance of redox balance, whereas
148 fermentation is characterized by an internal electron acceptor produced in intermediary
149 metabolism. In aerobic cell respiration, redox balance is maintained by O₂ as the electron acceptor.
150 (2) Compartmental coupling in vectorial OXPHOS contrasts to exclusively scalar substrate-level
151 phosphorylation in fermentation.

152
153 2. When measuring mitochondrial metabolism, the contribution of fermentation and other
154 cytosolic interactions must be excluded from analysis by disrupting the barrier function of the
155 plasma membrane. Selective removal or permeabilization of the plasma membrane yields
156 mitochondrial preparations—including isolated mitochondria, tissue and cellular preparations—
157 with structural and functional integrity. Subsequently, extramitochondrial concentrations of fuel
158 substrates, ADP, ATP, inorganic phosphate, and cations including H⁺ can be controlled to
159 determine mitochondrial function under a set of conditions defined as coupling control states. We
160 strive to incorporate an easily recognized and understood concept-driven terminology of
161 bioenergetics with explicit terms and symbols that define the nature of respiratory states.

162
163 3. Mitochondrial coupling states are defined according to the control of respiratory oxygen flux
164 by the protonmotive force, *pmF*, in an interaction of the electron transfer system generating the
165 *pmF* and the phosphorylation system utilizing the *pmF*. Capacities of OXPHOS and electron
166 transfer are measured at kinetically-saturating concentrations of fuel substrates, ADP and
167 inorganic phosphate, and O₂, or at optimal uncoupler concentrations, respectively, in the absence
168 of Complex IV inhibitors such as NO, CO, or H₂S. Respiratory capacity is a measure of the upper

169 boundary of the rate of respiration; it depends on the substrate type undergoing oxidation in a
170 mitochondrial pathway, and provides reference values for the diagnosis of health and disease.
171 Evaluation of the impact of evolutionary background, age, gender and sex, lifestyle and
172 environment represents a major challenge for mitochondrial respiratory physiology and
173 pathology.

174
175 4. Incomplete tightness of coupling, *i.e.*, some degree of uncoupling relative to the mitochondrial
176 pathway-dependent coupling stoichiometry, is a characteristic of energy-transformations across
177 membranes. Uncoupling is caused by a variety of physiological, pathological, toxicological,
178 pharmacological and environmental conditions that exert an influence not only on the proton leak
179 and cation cycling, but also on proton slip within the proton pumps and the structural integrity of
180 the mitochondria. A more loosely coupled state is induced by stimulation of mitochondrial
181 superoxide formation and the bypass of proton pumps. In addition, the use of protonophores
182 represents an experimental uncoupling intervention to assess the transition from a well-coupled
183 to a noncoupled state of mitochondrial respiration.

184
185 5. Respiratory oxygen consumption rates have to be carefully normalized to enable meta-analytic
186 studies beyond the question of a particular experiment. Therefore, all raw data on rates and
187 variables for normalization should be published in an open access data repository. Normalization
188 of rates for: (1) the number of objects (cells, organisms); (2) the volume or mass of the
189 experimental sample; and (3) the concentration of mitochondrial markers in the instrumental
190 chamber are sample-specific normalizations, which are distinguished from system-specific
191 normalization for the volume of the instrumental chamber (the measuring system).

192
193 6. The consistent use of terms and symbols facilitates transdisciplinary communication and will
194 support the further development of a collaborative database on bioenergetics and mitochondrial
195 physiology.

196

197 **1. Part 2. States and rates**

198

199 Mitochondria are the powerhouses of the cell with numerous morphological, physiological,
200 molecular, and genetic functions. Every study of mitochondrial health and disease faces **Evolution,**
201 **Age, Gender and sex, Lifestyle, and Environment (MitoEAGLE)** as essential background conditions
202 intrinsic to the individual person or cohort, species, tissue and to some extent even cell line. As a
203 large and coordinated group of laboratories and researchers, the mission of the global MitoEAGLE
204 Network is to generate the necessary scale, type, and quality of consistent data sets and conditions
205 to address this intrinsic complexity. Harmonization of experimental protocols and
206 implementation of a quality control and data management system are required to interrelate
207 results gathered across a spectrum of studies and to generate a rigorously monitored database
208 focused on mitochondrial respiratory function. In this way, researchers from a variety of
209 disciplines can compare their findings using clearly defined and accepted international standards.

210 With an emphasis on quality of research, published data can be useful far beyond the specific
211 question of a particular experiment. For example, collaborative data sets support the development
212 of open-access databases such as those for National Institutes of Health sponsored research in
213 genetics, proteomics, and metabolomics. Indeed, enabling meta-analysis is the most economic
214 way of providing robust answers to biological questions (Cooper *et al* 2009). However, the
215 reproducibility of quantitative results depend on accurate measurements under strictly-defined
216 conditions. Likewise, meaningful interpretation and comparability of experimental outcomes
217 requires harmonization of protocols between research groups at different institutes. In addition
218 to quality control, a conceptual framework is also required to standardise and harmonise
219 terminology and methodology. Vague or ambiguous jargon can lead to confusion and may convert
220 valuable signals to wasteful noise. For this reason, measured values must be expressed in standard
221 units for each parameter used to define mitochondrial respiratory function. A consensus on
222 fundamental nomenclature and conceptual coherence, however, are missing in the expanding
223 field of mitochondrial physiology. To fill this gap, the present communication provides an in-depth
224 review on harmonization of nomenclature and definition of technical terms, which are essential

225 to improve the awareness of the intricate meaning of current and past scientific vocabulary. This
226 is important for documentation and integration into data repositories in general, and quantitative
227 modelling in particular (Beard 2005).

228 In this review, we focus on coupling states and fluxes through metabolic pathways of aerobic
229 energy transformation in mitochondrial preparations in the attempt to establish a conceptually-
230 oriented nomenclature in bioenergetics and mitochondrial physiology in a series of
231 communications, prepared in the frame of the EU COST Action MitoEAGLE open to global bottom-
232 up input. [Reference to Part 1. Quantitative mitochondrial physiology. Mitochondria and bioblasts](#)
233

234 2. Coupling states and rates in mitochondrial preparations

235
236 *'Every professional group develops its own technical jargon for talking about matters of critical*
237 *concern ... People who know a word can share that idea with other members of their group, and*
238 *a shared vocabulary is part of the glue that holds people together and allows them to create a*
239 *shared culture'* (Miller 1991).
240

241 2.1. Cellular and mitochondrial respiration

242
243 **2.1.1. Aerobic and anaerobic catabolism and ATP turnover:** In respiration, electron transfer
244 is coupled to the phosphorylation of ADP to ATP, with energy transformation mediated by the
245 protonmotive force, pmF (**Figure 2**). Anabolic reactions are coupled to catabolism, both by ATP
246 as the intermediary energy currency and by small organic precursor molecules as building blocks
247 for biosynthesis (Diebold *et al* 2019). Glycolysis involves substrate-level phosphorylation of ADP
248 to ATP in fermentation without utilization of O_2 , studied mainly in living cells and organisms. Many
249 cellular fuel substrates are catabolized to acetyl-CoA or to glutamate, and further electron transfer
250 reduces nicotinamide adenine dinucleotide to NADH or flavin adenine dinucleotide to $FADH_2$.
251 Subsequent mitochondrial electron transfer to O_2 is coupled to proton translocation for the
252 control of the protonmotive force and phosphorylation of ADP (**Figure 1b and 1c**). In
253 contrast, extramitochondrial oxidation of fatty acids and amino acids proceeds partially in
254 peroxisomes without coupling to ATP production: acyl-CoA oxidase catalyzes the oxidation of
255 $FADH_2$ with electron transfer to O_2 ; amino acid oxidases oxidize flavin mononucleotide $FMNH_2$ or
256 $FADH_2$ (**Figure 1a**).

257 The plasma membrane separates the intracellular compartment including the cytosol, nucleus,
258 and organelles from the extracellular environment. Cell membranes include the plasma
259 membrane and organellar membranes. The plasma membrane consists of a lipid bilayer with
260 embedded proteins and attached organic molecules that collectively control the selective
261 permeability of ions, organic molecules, and particles across the cell boundary. The intact plasma
262 membrane prevents the passage of many water-soluble mitochondrial substrates and inorganic
263 ions—such as succinate, adenosine diphosphate (ADP) and inorganic phosphate (P_i) that must be
264 precisely controlled at kinetically-saturating concentrations for the analysis of mitochondrial
265 respiratory capacities (**Figure 2**). Respiratory capacities delineate, comparable to channel
266 capacity in information theory (Schneider 2006), the upper boundary of the rate of O_2
267 consumption measured in defined respiratory states. The intact plasma membrane limits the
268 scope of investigations into mitochondrial respiratory function in living cells, despite the activity
269 of solute carriers, *e.g.*, the sodium-dependent dicarboxylate transporter SLC13A3 and the sodium-
270 dependent phosphate transporter SLC20A2, which transport specific metabolites across the
271 plasma membrane of various cell types, and the availability of plasma membrane-permeable
272 succinate (Ehinger *et al* 2016). These limitations are overcome by the use of mitochondrial
273 preparations.
274

275 **2.1.2. Specification of biochemical dose:** Substrates, uncouplers, inhibitors, and other chemical
276 reagents are titrated to analyse cellular and mitochondrial function. Nominal concentrations of
277 these substances are usually reported as initial amount of substance concentration [$mol \cdot L^{-1}$] in the
278 incubation medium.

279 Kinetically-saturating conditions are evaluated by substrate kinetics to obtain the maximum
280 reaction velocity or maximum pathway flux, in contrast to solubility-saturated conditions. When
281 aiming at the measurement of kinetically-saturated processes—such as OXPHOS-capacities—the
282 concentrations for substrates can be chosen according to half-saturating substrate
283 concentrations, c_{50} , for metabolic pathways, or the Michaelis constant, K_m , for enzyme kinetics. In
284 the case of hyperbolic kinetics, only 80 % of maximum respiratory capacity is obtained at a
285 substrate concentration of four times the c_{50} , whereas substrate concentrations of 5, 9, 19 and 49
286 times the c_{50} are theoretically required for reaching 83 %, 90 %, 95 % or 98 % of the maximal rate
287 (Gnaiger 2001).

288 Other reagents are chosen to inhibit or alter a particular process. The amount of these
289 chemicals in an experimental incubation is selected to maximize effect, avoiding unacceptable off-
290 target consequences that would adversely affect the data being sought. Specifying the amount of
291 substance in an incubation as nominal concentration in the aqueous incubation medium can be
292 ambiguous (Doskey *et al* 2015), particularly for cations (TPP⁺; fluorescent dyes such as safranin,
293 TMRM; Chowdhury *et al* 2015) and lipophilic substances (oligomycin, uncouplers,
294 permeabilization agents; Doerrier *et al* 2018), which accumulate in the mitochondrial matrix or
295 in biological membranes, respectively. Generally, dose/exposure can be specified per unit of
296 biological sample, *i.e.*, (nominal moles of xenobiotic)/(number of cells) [$\text{mol}\cdot\text{cell}^{-1}$] or, as
297 appropriate, per mass of biological sample [$\text{mol}\cdot\text{kg}^{-1}$]. This approach to specification of
298 dose/exposure provides a scalable parameter that can be used to design experiments, help
299 interpret a wide variety of experimental results, and provide absolute information that allows
300 researchers worldwide to make the most use of published data (Doskey *et al* 2015).

301

302 2.2. Mitochondrial preparations

303

304 Mitochondrial preparations are defined as either isolated mitochondria or tissue and cellular
305 preparations in which the barrier function of the plasma membrane is disrupted. Since this entails
306 the loss of cell viability, mitochondrial preparations are not studied *in vivo*. In contrast to isolated
307 mitochondria and tissue homogenate preparations, mitochondria in permeabilized tissues and
308 cells are *in situ* relative to the plasma membrane. When studying mitochondrial preparations,
309 substrate-uncoupler-inhibitor-titration (SUIT) protocols are used to establish respiratory
310 coupling control states (CCS) and pathway control states (PCS) that provide reference values for
311 various output variables (**Table 1**). Physiological conditions *in vivo* deviate from these
312 experimentally obtained states; this is because kinetically-saturating concentrations, *e.g.*, of ADP,
313 oxygen (O_2 ; dioxygen) or fuel substrates, may not apply to physiological intracellular conditions.
314 Further information is obtained in studies of kinetic responses to variations in fuel substrate
315 concentrations, [ADP], or [O_2] in the range between kinetically-saturating concentrations and
316 anoxia (Gnaiger 2001).

317 The cholesterol content of the plasma membrane is high compared to mitochondrial
318 membranes (Korn 1969). Therefore, mild detergents—such as digitonin and saponin—can be
319 applied to selectively permeabilize the plasma membrane via interaction with cholesterol; this
320 allows free exchange of organic molecules and inorganic ions between the cytosol and the
321 immediate cell environment, while maintaining the integrity and localization of organelles,
322 cytoskeleton, and the nucleus. Application of permeabilization agents (mild detergents or toxins)
323 leads to washout of cytosolic marker enzymes—such as lactate dehydrogenase—and results in
324 the complete loss of cell viability (tested by nuclear staining using plasma membrane-
325 impermeable dyes), while mitochondrial function remains intact (tested by cytochrome *c*
326 stimulation of respiration). Digitonin concentrations have to be optimized according to cell
327 type, particularly since mitochondria from cancer cells contain significantly higher contents of
328 cholesterol in both membranes (Baggetto and Testa-Perussini, 1990). For example, a dose of
329 digitonin of $8 \text{ fmol}\cdot\text{cell}^{-1}$ ($10 \text{ pg}\cdot\text{cell}^{-1}$; $10 \mu\text{g}\cdot 10^{-6} \text{ cells}$) is optimal for permeabilization of
330 endothelial cells, and the concentration in the incubation medium has to be adjusted according to
331 the cell concentration (Doerrier *et al* 2018). Respiration of isolated mitochondria remains
332 unaltered after the addition of low concentrations of digitonin or saponin. In addition to

333 mechanical cell disruption during homogenization of tissue, permeabilization agents may be
334 applied to ensure permeabilization of all cells in tissue homogenates.

335 Suspensions of cells permeabilized in the respiration chamber and crude tissue homogenates
336 contain all components of the cell at highly dilute concentrations. All mitochondria are retained
337 in chemically-permeabilized mitochondrial preparations and crude tissue homogenates. In the
338 preparation of isolated mitochondria, however, the mitochondria are separated from other cell
339 fractions and purified by differential centrifugation, entailing the loss of mitochondria at typical
340 recoveries ranging from 30 % to 80 % of total mitochondrial content (Lai *et al* 2018). Using Percoll
341 or sucrose density gradients to maximize the purity of isolated mitochondria may compromise
342 the mitochondrial yield or structural and functional integrity. Therefore, mitochondrial isolation
343 protocols need to be optimized according to each study. The term *mitochondrial preparation*
344 neither includes living cells, nor submitochondrial particles and further fractionated
345 mitochondrial components.

346

347 2.3. Electron transfer pathways

348

349

349 Mitochondrial electron transfer (ET) pathways are fuelled by diffusion and transport of substrates
350 across the mtOM and mtIM. In addition, the mitochondrial electron transfer system (ETS) consists
351 of the matrix-ETS and membrane-ETS (**Figure 1b**). Upstream sections of ET-pathways converge
352 at the NADH-junction (N-junction). NADH is mainly generated in the tricarboxylic acid (TCA) cycle
353 and is oxidized by Complex I (CI), with further electron entry into the coenzyme Q-junction (Q-
354 junction). Similarly, succinate is formed in the TCA cycle and oxidized by CII to fumarate. CII is
355 part of both the TCA cycle and the ETS, and reduces FAD to FADH₂ with further reduction of
356 ubiquinone to ubiquinol downstream of the TCA cycle in the Q-junction. Thus FADH₂ is not a
357 substrate but is the product of CII, in contrast to erroneous metabolic maps shown in many
358 publications. β -oxidation of fatty acids (FA) supplies reducing equivalents via (1) FADH₂ as the
359 substrate of electron transferring flavoprotein complex (ETF); (2) acetyl-CoA generated by chain
360 shortening; and (3) NADH generated via 3-hydroxyacyl-CoA dehydrogenases. The ATP yield
361 depends on whether acetyl-CoA enters the TCA cycle, or is for example used in ketogenesis.

362 Selected mitochondrial catabolic pathways of electron transfer from the oxidation of fuel
363 substrates to the reduction of O₂ are stimulated by addition of fuel substrates to the mitochondrial
364 respiration medium after depletion of endogenous substrates (**Figure 1b**). Substrate
365 combinations and specific inhibitors of ET-pathway enzymes are used to obtain defined pathway
366 control states in mitochondrial preparations (Gnaiger 2020).

367

368 2.4. Respiratory coupling control

369

370

370 **2.4.1. Coupling:** In mitochondrial electron transfer, vectorial transmembrane proton flux is
371 coupled through the redox proton pumps CI, CIII and CIV to the catabolic flux of scalar reactions,
372 collectively measured as O₂ flux, J_{ko_2} (**Figure 1**). Thus mitochondria are elementary components
373 of energy transformation. Energy is a conserved quantity and cannot be lost or produced in any
374 internal process (First Law of Thermodynamics). Open and closed systems can gain or lose energy
375 only by external fluxes—by exchange with the environment. Therefore, energy can neither be
376 produced by mitochondria, nor is there any internal process without energy conservation. Exergy
377 or Gibbs energy ('free energy') is the part of energy that can potentially be transformed into work
378 under conditions of constant temperature and pressure. *Coupling* is the interaction of an
379 exergonic process (spontaneous, negative exergy change) with an endergonic process (positive
380 exergy change) in energy transformations which conserve part of the exergy change. Exergy is not
381 completely conserved, however, except at the limit of 100 % efficiency of energy transformation
382 in a coupled process. The exergy or Gibbs energy change that is not conserved by coupling is
383 irreversibly lost or dissipated, and is accounted for as the entropy change of the surroundings and
384 the system, multiplied by the temperature of the irreversible process.

385 Pathway control states (PCS) and coupling control states (CCS) are complementary, since
 386 mitochondrial preparations depend on (1) an exogenous supply of pathway-specific fuel
 387 substrates and oxygen, and (2) exogenous control of phosphorylation (**Figure 1**).
 388

389 **2.4.2. Phosphorylation, P_», and P_»/O₂ ratio:** Phosphorylation in the context of OXPHOS is
 390 defined as phosphorylation of ADP by P_i to form ATP. On the other hand, the term phosphorylation
 391 is used generally in many contexts, *e.g.*, protein phosphorylation. This provides the argument for
 392 introducing a symbol more discriminating and specific than P as used in the P/O ratio (phosphate
 393 to atomic oxygen ratio), where P indicates phosphorylation of ADP to ATP or GDP to GTP (**Figure**
 394 **1**): The symbol P_» indicates the endergonic (uphill) direction of phosphorylation ADP→ATP, and
 395 likewise P_« the corresponding exergonic (downhill) hydrolysis ATP→ADP. P_» refers mainly to
 396 electrontransfer phosphorylation but may also involve substrate-level phosphorylation as part of
 397 the TCA cycle (succinyl-CoA ligase, phosphoglycerate kinase) and phosphorylation of ADP
 398 catalyzed by pyruvate kinase, and of GDP phosphorylated by phosphoenolpyruvate
 399 carboxykinase. Transphosphorylation is performed by adenylate kinase, creatine kinase (mtCK),
 400 hexokinase and nucleoside diphosphate kinase. In isolated mammalian mitochondria, ATP
 401 production catalyzed by adenylate kinase (2 ADP ↔ ATP + AMP) proceeds without fuel substrates
 402 in the presence of ADP (Kömödi and Tretter 2017). Kinase cycles are involved in intracellular
 403 energy transfer and signal transduction for regulation of energy flux. The P_»/O₂ ratio (P_»/4 e⁻) is
 404 two times the 'P/O' ratio (P_»/2 e⁻). P_»/O₂ is a generalized symbol, not specific for reporting P_i
 405 consumption (P_i/O₂ flux ratio), ADP depletion (ADP/O₂ flux ratio), or ATP production (ATP/O₂
 406 flux ratio). The mechanistic P_»/O₂ ratio—or P_»/O₂ stoichiometry—is calculated from the proton-
 407 to-O₂ and proton-to-phosphorylation coupling stoichiometries (**Figure 1c**):

$$409 \quad P_{\gg}/O_2 = \frac{H_{\text{pos}}^+/O_2}{H_{\text{neg}}^+/P_{\gg}} \quad (1)$$

410
 411 The H⁺_{pos}/O₂ coupling stoichiometry (referring to the full four electron reduction of O₂) depends
 412 on the relative involvement of the three coupling sites (respiratory Complexes CI, CIII and CIV) in
 413 the catabolic ET-pathway from reduced fuel substrates (electron donors) to the reduction of O₂
 414 (electron acceptor). This varies with: (1) a bypass of CI by single or multiple electron input into
 415 the Q-junction; and (2) a bypass of CIV by involvement of alternative oxidases, AOX. AOX are
 416 expressed in all plants, some fungi, many protists, and several animal phyla, but are not expressed
 417 in vertebrate mitochondria (McDonald *et al* 2009).
 418

419 The H⁺_{pos}/O₂ coupling stoichiometry equals 12 in the ET-pathways involving CIII and CIV as
 420 proton pumps, increasing to 20 for the NADH-pathway through CI (**Figure 1b**). A general
 421 consensus on H⁺_{pos}/O₂ stoichiometries, however, remains to be reached (Hinkle 2005; Wikström
 422 and Hummer 2012; Sazanov 2015). The H⁺_{neg}/P_» coupling stoichiometry (3.7; **Figure 1b**) is the
 423 sum of 2.7 H⁺_{neg} required by the F₁F₀-ATPase of vertebrate and most invertebrate species (Watt
 424 *et al* 2010) and the proton balance in the translocation of ADP, ATP and P_i (**Figure 1c**). Taken
 425 together, the mechanistic P_»/O₂ ratio is calculated at 5.4 and 3.3 for the N- and S-pathway,
 426 respectively (Eq. 1). The corresponding classical P_»/O ratios (referring to the 2 electron reduction
 427 of 0.5 O₂) are 2.7 and 1.6 (Watt *et al* 2010), in agreement with the measured P_»/O ratio for
 428 succinate of 1.58 ± 0.02 (Gnaiger *et al* 2000).
 429

430 **2.4.3. Uncoupling:** The effective P_»/O₂ flux ratio ($Y_{P_{\gg}/O_2} = J_{P_{\gg}}/J_{kO_2}$) is diminished relative to the
 431 mechanistic P_»/O₂ ratio by intrinsic and extrinsic uncoupling or dyscoupling (**Figure 3**). This is
 432 distinct from switching between mitochondrial pathways that involve fewer than three proton
 433 pumps ('coupling sites': Complexes CI, CIII and CIV), bypassing CI through multiple electron
 434 entries into the Q-junction, or bypassing CIII and CIV through AOX (**Figure 1b**). Reprogramming
 435 of mitochondrial pathways leading to different types of substrates being oxidized may be
 436 considered as a switch of gears (changing the stoichiometry by altering the substrate that is
 437 oxidized) rather than uncoupling (loosening the tightness of coupling relative to a fixed
 438 stoichiometry). In addition, Y_{P_{\gg}/O_2} depends on several experimental conditions of flux control,

439 increasing as a hyperbolic function of [ADP] to a maximum value (Gnaiger 2001). Uncoupling of
440 mitochondrial respiration is a general term comprising diverse mechanisms (Figure 3):

- 441
442 1. Proton leak across the mtIM from the positive to the negative compartment (H^+ leak-
443 uncoupled);
444 2. Cycling of other cations, strongly stimulated by mtPT; comparable to the use of protonophores,
445 cation cycling is experimentally induced by valinomycin in the presence of K^+
446 3. Decoupling by proton slip in the redox proton pumps (CI, CIII and CIV) when protons are
447 effectively not pumped in the ETS, or are not driving phosphorylation (F_1F_0 -ATPase)
448 4. Loss of vesicular (compartmental) integrity when electron transfer is uncoupled
449 5. Electron leak in the loosely coupled univalent reduction of O_2 to superoxide ($O_2^{\cdot-}$; superoxide
450 anion radical)

451
452 Differences of terms—uncoupled vs. noncoupled—are easily overlooked, although they relate
453 to different meanings of uncoupling (Table 2 and Figure 3).

454

455 2.5. Coupling states and respiratory rates

456

457 To extend the classical nomenclature on mitochondrial coupling states (Section 2.6) by a concept-
458 driven terminology that explicitly incorporates information on the meaning of respiratory states,
459 the terminology must be general and not restricted to any particular experimental protocol or
460 mitochondrial preparation (Gnaiger 2009). Diagnostically meaningful and reproducible
461 conditions are defined for measuring mitochondrial function and respiratory capacities of core
462 energy metabolism. Standard respiratory coupling states are obtained while maintaining a
463 defined ET-pathway state with constant fuel substrates and inhibitors of specific branches of the
464 ET-pathway. Concept-driven nomenclature aims at mapping the meaning and concept behind the
465 words and acronyms onto the forms of words and acronyms (Miller 1991). The focus of concept-
466 driven nomenclature is primarily the conceptual *why*, along with clarification of the experimental
467 *how* (Table 1).

468

469 **LEAK:** The contribution of intrinsically uncoupled O_2 consumption is studied by preventing the
470 stimulation of phosphorylation either in the absence of ADP or by inhibition of the
471 phosphorylation-pathway. The corresponding states are collectively classified as LEAK-states
472 when O_2 consumption compensates mainly for ion leaks, including the proton leak.

473 **OXPHOS:** The ET- and phosphorylation-pathways comprise coupled segments of the OXPHOS-
474 system and provide reference values of respiratory capacities. The OXPHOS-capacity is
475 measured at kinetically-saturating concentrations of ADP and P_i .

476 **ET:** Compared to OXPHOS-capacity, the oxidative ET-capacity reveals the limitation of OXPHOS-
477 capacity mediated by the phosphorylation-pathway. By application of external uncouplers, ET-
478 capacity is measured as noncoupled respiration. The three coupling states, LEAK, OXPHOS, and
479 ET are shown schematically with the corresponding respiratory rates, abbreviated as *L*, *P*, and
480 *E*, respectively (Figure 2). We distinguish between metabolic *pathways* and metabolic *states*
481 with the corresponding metabolic *rates*; for example: ET-pathways, ET-states, and ET-
482 capacities, *E*, respectively (Table 1). The protonmotive force, *pmF*, is *maximum* in the LEAK-
483 state of coupled mitochondria, driven by LEAK-respiration at a minimum back-flux of cations
484 to the matrix side, *high* in the OXPHOS-state when it drives phosphorylation, and *very low* in
485 the ET-state when uncouplers short-circuit the proton cycle (Table 1).

486

487 **2.5.1. LEAK-state (Figure 4a):** The LEAK-state is defined as a state of mitochondrial respiration
488 when O_2 flux mainly compensates for ion leaks in the absence of ATP synthesis, at kinetically-
489 saturating concentrations of O_2 , respiratory fuel substrates and P_i . LEAK-respiration is measured
490 to obtain an estimate of intrinsic uncoupling without addition of an experimental uncoupler: (1)
491 in the absence of adenylates, *i.e.*, AMP, ADP and ATP; (2) after depletion of ADP at a maximum
492 ATP/ADP ratio; or (3) after inhibition of the phosphorylation-pathway by inhibitors of F_1F_0 -
493 ATPase (oligomycin), or adenine nucleotide translocase (carboxyatractyloside). Adjustment of

494 the nominal concentration of these inhibitors to the concentration of biological sample applied
495 can minimize or avoid inhibitory side-effects exerted on ET-capacity or even some dyscoupling.
496 The chelator EGTA is added to mt-respiration media to bind free Ca^{2+} , thus limiting cation cycling.
497 The LEAK-rate is a function of respiratory state, hence it depends on the (1) barrier function of
498 the mtIM ('leakiness'), (2) electrochemical potential differences and concentration differences
499 across the mtIM, and (3) H^+/O_2 ratio of the ET-pathway (**Figure 1b**).

- 500 • **Proton leak and uncoupled respiration:** The intrinsic proton leak is the *uncoupled* leak
501 current of protons in which protons diffuse across the mtIM in the dissipative direction of the
502 downhill protonmotive force without coupling to phosphorylation (**Figure 4a**). The proton
503 leak flux depends non-linearly on the protonmotive force (Garlid *et al* 1989; Divakaruni and
504 Brand 2011), which is a temperature-dependent property of the mtIM and may be enhanced
505 due to possible contamination by free fatty acids. Inducible uncoupling mediated by
506 uncoupling protein 1 (UCP1) is physiologically controlled, *e.g.*, in brown adipose tissue. UCP1
507 is a member of the
508 mitochondrial carrier family that is involved in the translocation of protons across the mtIM
509 (Jezek *et al* 2018). Consequently, this short-circuit lowers the pmF and stimulates electron
510 transfer, respiration, and heat dissipation in the absence of phosphorylation of ADP.
- 511 • **Cation cycling:** There can be other cation contributors to leak current including calcium and
512 probably magnesium. Calcium influx is balanced by mitochondrial $\text{Na}^+/\text{Ca}^{2+}$ or $\text{H}^+/\text{Ca}^{2+}$
513 exchange, which is balanced by Na^+/H^+ or K^+/H^+ exchanges. This is another effective
514 uncoupling mechanism different from proton leak (**Table 2**).
- 515 • **Proton slip and decoupled respiration:** Proton slip is the *decoupled* process in which protons
516 are only partially translocated by a redox proton pump of the ET-pathways and slip back to the
517 original vesicular compartment. The proton leak is the dominant contributor to the overall leak
518 current in mammalian mitochondria incubated under physiological conditions at 37 °C,
519 whereas proton slip increases at lower experimental temperature (Canton *et al* 1995). Proton
520 slip can also happen in association with the F_1F_0 -ATPase, in which the proton slips downhill
521 across the pump to the matrix without contributing to ATP synthesis. In each case, proton slip
522 is a property of the proton pump and increases with the pump turnover rate.
- 523 • **Electron leak and loosely coupled respiration:** Superoxide production by the ETS leads to a
524 bypass of redox proton pumps and correspondingly lower $\text{P}\gg/\text{O}_2$ ratio. This depends on the
525 actual site of electron leak and the scavenging of hydrogen peroxide by cytochrome *c*, whereby
526 electrons may re-enter the ETS with proton translocation by CIV.
- 527 • **Dyscoupled respiration:** Mitochondrial injuries may lead to *dyscoupling* as a pathological or
528 toxicological cause of *uncoupled* respiration. Dyscoupling may involve any type of uncoupling
529 mechanism, *e.g.*, opening the mtPT pore. Dyscoupled respiration is distinguished from
530 experimentally induced *noncoupled* respiration in the ET-state (**Table 2**).
- 531 • **Protonophore titration and noncoupled respiration:** Protonophores are uncouplers which
532 are titrated to obtain maximum *noncoupled* respiration as a measure of ET-capacity.
- 533 • **Loss of compartmental integrity and acoupled respiration:** Electron transfer and catabolic
534 O_2 flux proceed without compartmental proton translocation in disrupted mitochondrial
535 fragments. Such fragments are an artefact of mitochondrial isolation, and may not fully fuse to
536 re-establish structurally intact mitochondria. Loss of mtIM integrity, therefore, is the cause of
537 acoupled respiration, which is a nonvectorial dissipative process without control by the
538 protonmotive force.

539
540 **2.5.2. OXPHOS-state (Figure 4b):** The OXPHOS-state is defined as the respiratory state with
541 kinetically-saturating concentrations of O_2 , respiratory and phosphorylation substrates, and
542 absence of exogenous uncoupler, which provides an estimate of the maximal respiratory capacity
543 in the OXPHOS-state for any given ET-pathway state. Respiratory capacities at kinetically-
544 saturating substrate concentrations provide reference values or upper limits of performance,
545 aiming at the generation of data sets for comparative purposes. Physiological activities and effects
546 of substrate kinetics can be evaluated relative to the OXPHOS-capacity.

547 As discussed previously, 0.2 mM ADP does not kinetically-saturate flux in isolated
548 mitochondria (Gnaiger 2001; Puchowicz *et al* 2004); greater [ADP] is required, particularly in
549 permeabilized muscle fibers and cardiomyocytes, to overcome limitations by intracellular
550 diffusion and by the reduced conductance of the mtOM (Jepihhina *et al* 2011; Illaste *et al* 2012;
551 Simson *et al* 2016), either through interaction with tubulin (Rostovtseva *et al* 2008) or other
552 intracellular structures (Birkedal *et al* 2014). In addition, kinetically-saturating ADP
553 concentrations need to be evaluated under different experimental conditions such as temperature
554 (Lemieux *et al* 2017) and with different animal models (Blier and Guderley 1993). In
555 permeabilized muscle fiber bundles of high respiratory capacity, the apparent K_m for ADP
556 increases up to 0.5 mM (Saks *et al* 1998), consistent with experimental evidence that >90 %
557 kinetic saturation is reached only at >5 mM ADP (Pesta and Gnaiger 2012). Similar ADP
558 concentrations are also required for accurate determination of OXPHOS-capacity in human
559 clinical cancer samples and permeabilized cells (Klepinin *et al* 2016; Koit *et al* 2017). 2.5 to 5 mM
560 ADP is sufficient to obtain the actual OXPHOS-capacity in many types of permeabilized tissue and
561 cell preparations, but experimental validation is required in each specific case.
562

563 **2.5.3. Electron transfer-state (Figure 4c):** O_2 flux determined in the ET-state yields an estimate
564 of ET-capacity. The ET-state is defined as the *noncoupled* state with kinetically-saturating
565 concentrations of O_2 , respiratory substrate and optimum exogenous uncoupler concentration for
566 maximum O_2 flux. Uncouplers are weak lipid-soluble acids which function as protonophores.
567 These disrupt the barrier function of the mtIM and thus short-circuit the protonmotive system,
568 functioning like a clutch in a mechanical system. As a consequence of the nearly collapsed
569 protonmotive force, the driving force is insufficient for phosphorylation, and $J_{P_s} = 0$. The most
570 frequently used uncouplers are carbonyl cyanide *m*-chloro phenyl hydrazone (CCCP), carbonyl
571 cyanide *p*-trifluoromethoxyphenylhydrazone (FCCP), or dinitrophenol (DNP). Stepwise titration
572 of uncouplers stimulates respiration up to or above the level of O_2 consumption rates in the
573 OXPHOS-state; respiration is inhibited, however, above optimum uncoupler concentrations
574 (Mitchell 2011). Data obtained with a single dose of uncoupler must be evaluated with caution,
575 particularly when a fixed uncoupler concentration is used in studies exploring a treatment or
576 disease that may alter the mitochondrial content or mitochondrial sensitivity to inhibition by
577 uncouplers. There is a need for new protonophoric uncouplers that drive maximal respiration
578 across a broad dosing range and do not inhibit respiration at high concentrations (Kenwood *et al*
579 2013). The effect on ET-capacity of the reversed function of F_1F_0 -ATPase (J_{P_s} ; **Figure 4c**) can be
580 evaluated in the presence and absence of extramitochondrial ATP.
581

582 **2.5.4. ROX state:** The state of residual O_2 consumption, ROX, is not a coupling state, but is relevant
583 to assess respiratory function (**Overview**). The rate of residual oxygen consumption, *Rox*, is
584 defined as O_2 consumption due to oxidative reactions measured after inhibition of ET with
585 rotenone, malonic acid and antimycin A. Cyanide and azide inhibit not only CIV but catalase and
586 several peroxidases involved in *Rox*. High concentrations of antimycin A, but not rotenone or
587 cyanide, inhibit peroxisomal acyl-CoA oxidase and D-amino acid oxidase (Vamecq *et al* 1987). *Rox*
588 represents a baseline used to correct respiration measured in defined coupling control states. *Rox*-
589 corrected *L*, *P* and *E* are not only lower than total fluxes, but also change the flux control ratios *L/P*
590 and *L/E*. *Rox* is not necessarily equivalent to non-mitochondrial reduction of O_2 , considering O_2 -
591 consuming reactions in mitochondria that are not related to ET—such as O_2 consumption in
592 reactions catalyzed by monoamine oxidases (type A and B), monooxygenases (cytochrome P450
593 monooxygenases), dioxygenases (trimethyllysine dioxygenase), and several hydroxylases. Isolated
594 mitochondrial fractions, especially those obtained from liver, may be contaminated by
595 peroxisomes, as shown by transmission electron microscopy. This fact makes the exact
596 determination of mitochondrial O_2 consumption and mitochondria-associated generation of
597 reactive oxygen species complicated (Schönfeld *et al* 2009; Speijer 2016; **Figure 1**). The
598 variability of ROX-linked O_2 consumption needs to be studied in relation to non-ET enzyme
599 activities, availability of specific substrates, O_2 concentration, and electron leakage leading to the
600 formation of reactive oxygen species.

601
602 **2.5.5. Quantitative relations:** E may exceed or be equal to P . $E > P$ is observed in many types of
603 mitochondria, varying between species, tissues and cell types (Gnaiger 2009). $E - P$ is the ET-excess
604 capacity pushing the phosphorylation-flux to the limit of its capacity for utilizing the protonmotive
605 force (**Figure 2**). In addition, the magnitude of $E - P$ depends on the tightness of respiratory
606 coupling or degree of uncoupling, since an increase of L causes P to increase towards the limit of
607 E (Lemieux *et al* 2011). The ET-excess capacity, $E - P$, therefore, provides a sensitive diagnostic
608 indicator of specific injuries of the phosphorylation-pathway, under conditions when E remains
609 constant but P declines relative to controls. Substrate cocktails supporting simultaneous
610 convergent electron transfer to the Q-junction for reconstitution of TCA cycle function establish
611 pathway control states with high ET-capacity, and consequently increase the sensitivity of the $E -$
612 P assay.

613 E cannot theoretically be lower than P . $E < P$ must be discounted as an artefact, which may be
614 caused experimentally by: (1) loss of oxidative capacity during the time course of the
615 respirometric assay, since E is measured subsequently to P ; (2) using insufficient uncoupler
616 concentrations; (3) using high uncoupler concentrations which inhibit ET (Gnaiger 2008); (4) high
617 oligomycin concentrations applied for measurement of L before titrations of uncoupler, when
618 oligomycin exerts an inhibitory effect on E . On the other hand, the ET-excess capacity is
619 overestimated if kinetically non-saturating [ADP] or [P_i] are used. See State 3 in the next section.

620 The net OXPHOS-capacity is calculated by subtracting L from P (**Figure 2**). The net $P \gg O_2$
621 equals $P \gg / (P - L)$, wherein the dissipative LEAK component in the OXPHOS-state may be
622 overestimated. This can be avoided by measuring LEAK-respiration in a state when the
623 protonmotive force is adjusted to its slightly lower value in the OXPHOS-state by titration of an
624 ET-inhibitor (Divakaruni and Brand 2011). Any turnover-dependent components of proton leak
625 and slip, however, are underestimated under these conditions (Garlid *et al* 1993). In general, it is
626 inappropriate to use the term *ATP production* or *ATP turnover* for the difference of O_2 flux
627 measured in the OXPHOS- and LEAK-states. $P - L$ is the upper limit of OXPHOS-capacity that is freely
628 available for ATP production (corrected for LEAK-respiration) and is fully coupled to
629 phosphorylation with a maximum mechanistic stoichiometry (**Figure 2**).

630 LEAK-respiration and OXPHOS-capacity depend on (1) the tightness of coupling under the
631 influence of the respiratory uncoupling mechanisms (**Figure 3**), and (2) the coupling
632 stoichiometry, which varies as a function of the substrate type undergoing oxidation in ET-
633 pathways with either two or three coupling sites (**Figure 1b**). When substrate cocktails are used
634 supporting the convergent NADH- and succinate-pathways simultaneously, the relative
635 contribution of ET-pathways with three or two coupling sites cannot be controlled
636 experimentally, is difficult to determine, and may shift in transitions between LEAK-, OXPHOS-
637 and ET-states (Gnaiger 2020). Under these experimental conditions, we cannot separate the
638 tightness of coupling *versus* coupling stoichiometry as the mechanisms of respiratory control in a
639 shift of L/P ratios. The tightness of coupling and fully coupled O_2 flux, $P - L$ (**Table 2**), therefore, are
640 obtained from measurements of coupling control of LEAK-respiration, OXPHOS- and ET-
641 capacities in well-defined pathway states, using either pyruvate and malate as substrates or the
642 classical succinate and rotenone substrate-inhibitor combination (**Figure 1b**).

643
644 **2.5.6. The steady-state:** Mitochondria represent a thermodynamically open system in non-
645 equilibrium states of biochemical energy transformation. State variables (protonmotive force;
646 redox states) and metabolic *rates* (fluxes) are measured in defined mitochondrial respiratory
647 states. Steady-states can be obtained only in open systems, in which changes by internal
648 transformations, *e.g.*, O_2 consumption, are instantaneously compensated for by external fluxes
649 across the system boundary, *e.g.*, O_2 supply, preventing a change of O_2 concentration in the system
650 (Gnaiger 1993b). Mitochondrial respiratory states monitored in closed systems satisfy the criteria
651 of pseudo-steady states for limited periods of time, when changes in the system (concentrations
652 of O_2 , fuel substrates, ADP, P_i , H^+) do not exert significant effects on metabolic fluxes (respiration,
653 phosphorylation). Such pseudo-steady states require respiratory media with sufficient buffering

654 capacity and substrates maintained at kinetically-saturating concentrations, and thus depend on
655 the kinetics of the processes under investigation.

656

657 2.6. Classical terminology for isolated mitochondria

658 *'When a code is familiar enough, it ceases appearing like a code; one forgets that there is a*
659 *decoding mechanism. The message is identical with its meaning'* (Hofstadter 1979).

660

661 Chance and Williams (1955; 1956) introduced five classical states of mitochondrial respiration
662 and cytochrome redox states. **Table 3** shows a protocol with isolated mitochondria in a closed
663 respirometric chamber, defining a sequence of respiratory states. States and rates are not
664 distinguished in this nomenclature.

665

666 **2.6.1. State 1** is obtained after addition of isolated mitochondria to air-saturated
667 isoosmotic/isotonic respiration medium containing P_i, but no fuel substrates and no adenylates.

668

669 **2.6.2. State 2** is induced by addition of a 'high' concentration of ADP (typically 100 to 300 μM),
670 which stimulates respiration transiently on the basis of endogenous fuel substrates and
671 phosphorylates only a small portion of the added ADP. State 2 is then obtained at a low respiratory
672 activity limited by exhausted endogenous fuel substrate availability (**Table 3**). If addition of
673 specific inhibitors of respiratory complexes such as rotenone does not cause a further decline of
674 O₂ flux, State 2 is equivalent to the ROX state (**Table 1**). Undefined endogenous fuel substrates are
675 a confounding factor of pathway control, contributing to the effect of subsequently externally
676 added substrates and inhibitors. In an alternative sequence of titration steps, the second state is
677 induced by addition of fuel substrate without ADP or ATP (Estabrook 1967). In contrast to the
678 original State 2 defined in **Table 1** as a ROX state, the alternative 'State 2' is a LEAK-state with
679 L(n). Some researchers have called this condition as 'pseudostate 4'.

680

681 **2.6.3. State 3** is the state stimulated by addition of fuel substrates while the ADP concentration in
682 the original State 2 is still high (**Table 3**) and supports coupled energy transformation. 'High ADP'
683 is a concentration of ADP specifically selected to allow the measurement of State 3 to State 4
684 transitions of isolated mitochondria in a closed respirometric chamber. Repeated ADP titration
685 re-establishes State 3 at 'high ADP'. Starting at O₂ concentrations near air-saturation (193 or 238
686 μM O₂ at 37 °C or 25 °C and sea level at 1 atm or 101.32 kPa, and an oxygen solubility of respiration
687 medium at 0.92 times that of pure water; Forstner and Gnaiger 1983), the total ADP concentration
688 added must be low enough (typically 100 to 300 μM) to allow phosphorylation to ATP at a coupled
689 O₂ flux that does not lead to O₂ depletion during the transition to State 4. In contrast, kinetically-
690 saturating ADP concentrations usually are 10-fold higher than 'high ADP', e.g., 2.5 mM in isolated
691 mitochondria. The abbreviation State 3u is occasionally used in bioenergetics, to indicate the state
692 of respiration after titration of an uncoupler, without sufficient emphasis on the fundamental
693 difference between OXPHOS-capacity (*well-coupled* with an endogenous uncoupled component)
694 and ET-capacity (*noncoupled*).

695

696 **2.6.4. State 4** is a LEAK-state that is obtained only if the mitochondrial preparation is intact and
697 well-coupled. Depletion of ADP by phosphorylation to ATP causes a decline of O₂ flux in the
698 transition from State 3 to State 4. Under the conditions of State 4, a maximum protonmotive force
699 and high ATP/ADP ratio are maintained. The gradual decline of Y_{P_o/O₂} towards diminishing [ADP]
700 at State 4 must be taken into account for calculation of P_o/O₂ ratios (Gnaiger 2001). State 4
701 respiration, L(T) (**Table 1**), reflects intrinsic proton leak and ATP hydrolysis activity. O₂ flux in
702 State 4 is an overestimation of LEAK-respiration if the contaminating ATP hydrolysis activity
703 recycles some ATP to ADP, J_{P_o}, which stimulates respiration coupled to phosphorylation, J_{P_o} > 0.
704 Some degree of mechanical disruption and loss of mitochondrial integrity allows the exposed
705 mitochondrial F₁F₀-ATPases to hydrolyze the ATP synthesized by the fraction of coupled
706 mitochondria. This can be tested by inhibition of the phosphorylation-pathway using oligomycin,
707 ensuring that J_{P_o} = 0 (State 4o). On the other hand, the State 4 respiration reached after exhaustion

708 of added ADP is a more physiological condition, *i.e.*, presence of ATP, ADP and even AMP.
709 Sequential ADP titrations re-establish State 3, followed by State 3 to State 4 transitions while
710 sufficient O₂ is available. Anoxia may be reached, however, before exhaustion of ADP (State 5).

711
712 **2.6.5. State 5** 'may be obtained by antimycin A treatment or by anaerobiosis' (Chance and Williams,
713 1955). These definitions give State 5 two different meanings: ROX or anoxia. Anoxia is obtained
714 after exhaustion of O₂ in a closed respirometric chamber. Diffusion of O₂ from the surroundings
715 into the aqueous solution may be a confounding factor preventing complete anoxia (Gnaiger
716 2001).

717 In **Table 3**, only States 3 and 4 are coupling control states, with the restriction that rates in
718 State 3 may be limited kinetically by non-saturating ADP concentrations.

719
720 *2.7. Control and regulation*

721
722 **Reference to Part 1. Quantitative mitochondrial physiology. Mitochondria and bioblasts**

723 724 **3. What is a rate?**

725
726 The term *rate* is not adequately defined to be useful for reporting data. Normalization of rates
727 leads to a diversity of formats. Application of common and defined units is required for direct
728 transfer of reported results into a data repository. The second [s] is the SI unit for the base
729 quantity *time*. It is also the standard time-unit used in solution chemical kinetics.

730 The inconsistency of the meanings of rate becomes apparent when considering Galileo Galilei's
731 famous principle, that 'bodies of different weight all fall at the same rate (have a constant
732 acceleration)' (Coopersmith 2010). A rate may be an extensive quantity, which is a *flow*, *I*, when
733 expressed per *object* (per number of cells or organisms) or per chamber (per instrumental
734 system). *System* is defined as the open or closed chamber of the measuring device. A rate is a *flux*,
735 *J*, when expressed as a size-specific quantity (**Figure 5A; Box 1**).

736

737 **Box 1: Metabolic flows and fluxes: vectorial, vectorial, and scalar**

738
739 Flow is an extensive quantity (*I*; per system), distinguished from flux as a size-specific quantity (*J*;
740 per system size). *Flows*, *I*_{tr}, are defined for all transformations as extensive quantities. This is a
741 generalization derived from electrical terms: Electric charge per unit time is electric flow or
742 current, $I_{el} = dQ_{el} \cdot dt^{-1}$ [$A \equiv C \cdot s^{-1}$]. When dividing *I*_{el} by size of the system (cross-sectional area of a
743 'wire'), we obtain flux as a size-specific quantity; this is the current density (surface-density of
744 flow) perpendicular to the direction of flux, $J_{el} = I_{el} \cdot A^{-1}$ [$A \cdot m^{-2}$] (Cohen *et al* 2008). Fluxes with
745 *spatial* geometric direction and magnitude are *vectors*. Vector and scalar *fluxes* are related to flows
746 as $J_{tr} = I_{tr} \cdot A^{-1}$ [$mol \cdot s^{-1} \cdot m^{-2}$] and $J_{tr} = I_{tr} \cdot V^{-1}$ [$mol \cdot s^{-1} \cdot m^{-3}$], expressing flux as an area-specific vector or
747 volume-specific vectorial or scalar quantity, respectively (Gnaiger 1993b). We use the metre-
748 kilogram-second-ampere (MKSA) international system of units (SI) for general cases ([m], [kg],
749 [s] and [A]), with decimal SI prefixes for specific applications (**Table 4**).

750 We suggest defining: (1) *vectorial* fluxes, which are translocations as functions of *gradients* with
751 direction in geometric space in continuous systems; (2) *vectorial* fluxes, which describe
752 translocations in discontinuous systems and are restricted to information on *compartmental*
753 *differences* (transmembrane proton flux); and (3) *scalar* fluxes, which are localized
754 transformations without translocation, such as chemical reactions in a homogenous system
755 (catabolic O₂ flux, *J*_{kO₂}).

756

- 757 • **Extensive quantities:** An extensive quantity increases proportionally with system size. For
758 example, mass and volume are extensive quantities. Flow is an extensive quantity. The
759 magnitude of an extensive quantity is completely additive for non-interacting subsystems. The
760 magnitude of these quantities depends on the extent or size of the system (Cohen *et al* 2008).

- 761 • **Size-specific quantities:** ‘The adjective *specific* before the name of an extensive quantity is
 762 often used to mean *divided by mass*’ (Cohen *et al* 2008). The term *specific* has different
 763 meanings in three particular contexts: (1) In the system-paradigm, (a) mass-specific flux is flow
 764 divided by mass of the system (the mass of everything contained in the instrumental chamber
 765 or reactor). (b) Rates are frequently expressed as volume-specific flux (volume of the
 766 instrumental chamber). A mass-specific or volume-specific quantity is independent of the
 767 extent of non-interacting homogenous subsystems. (2) In the context of *sample size*, tissue-
 768 specific quantities are related to the mass or volume of the sample in contrast to the mass or
 769 volume of the *system* (e.g., muscle mass-specific or cell volume-specific normalization; **Figure**
 770 **5**). (3) An entirely different meaning is implied in the context of *sample type* (e.g., muscle-
 771 specific compared to brain-specific properties).
- 772 • **Intensive quantities:** In contrast to size-specific properties, forces are intensive quantities
 773 defined as the change of an extensive quantity per advancement of an energy transformation
 774 (Gnaiger 1993b).
- 775 • **Formats:** The quantity of a sample X can be expressed in different formats. n_X , N_X , and m_X are
 776 the molar amount, number, and mass of X , respectively. When different formats are indicated
 777 in symbols of derived quantities, the format (\underline{n} , \underline{N} , \underline{m}) is shown as a subscript (*underlined italic*),
 778 such as in $I_{O_2/\underline{N}X}$ and $J_{O_2/\underline{m}X}$. As of 2019 May 20, the definition of the SI unit mole [mol] is based
 779 on a natural constant, namely Avogadro’s constant: one mole contains exactly $6.02214076 \cdot 10^{23}$
 780 elementary entities, in contrast to the former definition in terms of the number of atoms in the
 781 mass of 0.012 kilogram of carbon 12 (Gibney 2018). Metabolic oxygen flow and flux are
 782 expressed in the molar format, n_{O_2} [mol], but in the volume format, V_{O_2} [m³], in ergometry.
 783 These formats are distinguished as $J_{\underline{n}O_2/\underline{m}X}$ and $J_{V\underline{O}_2/\underline{m}X}$, respectively, for mass-specific flux.
 784 Further examples are given in **Table 4** and **Figure 5**.

785 4. Normalization of rate per sample

786 The challenges of measuring mitochondrial respiratory flux are matched by those of
 787 normalization. Normalization (**Table 4**) is guided by physicochemical principles, methodological
 788 considerations, and conceptual strategies (**Figure 5**).

789 4.1. Flow: per object

790 **4.1.1. Number concentration, C_{NX} :** Normalization per sample concentration is routinely required
 791 to report respiratory data. C_{NX} is the experimental number concentration of sample X . In the case
 792 of animals N_X is the number of organisms in the chamber, e.g., nematodes, $C_{NX} = N_X \cdot V^{-1}$ [x·L⁻¹].
 793 Similarly, the number of cells per chamber volume is the number concentration of cells, $C_{Nce} =$
 794 $N_{ce} \cdot V^{-1}$ [x·L⁻¹], where N_{ce} is the number of cells in the chamber (**Table 4**).

795 **4.1.2. Flow per object, $I_{O_2/\underline{N}X}$:** O₂ flow per cell is calculated from volume-specific O₂ flux, J_{V,O_2}
 796 [nmol·s⁻¹·L⁻¹] (per V of the instrumental chamber [L]), divided by the number concentration of
 797 cells. The total cell count is the sum of viable and dead cells, $N_{ce} = N_{vce} + N_{dce}$ (**Table 5**). The cell
 798 viability index, $VI = N_{vce} \cdot N_{ce}^{-1}$, is the ratio of the number of viable cells, N_{vce} , per total number of
 799 living cells in the population. After experimental permeabilization, all cells are permeabilized, N_{pce}
 800 $= N_{ce}$. The cell viability index can be used to normalize respiration for the number of cells that have
 801 been viable before experimental permeabilization, $I_{O_2/\underline{N}vce} = I_{O_2/\underline{N}ce} \cdot VI^{-1}$, considering that
 802 mitochondrial respiratory dysfunction in dead cells should be eliminated as a confounding factor.

803 4.2. Size-specific flux: per sample size

804 **4.2.1. Sample concentration, C_{mX} :** Considering permeabilized tissue, homogenate or cells as the
 805 sample, X , the sample mass is m_X [mg], which is frequently measured as wet or dry mass, m_w or m_d [mg],
 806 respectively, or as mass of protein, m_{Protein} . The sample concentration is the mass of the subsample per
 807
 808
 809
 810
 811
 812
 813

814 volume of the instrumental chamber, $C_{mX} = m_X \cdot V^{-1}$ [$\text{g} \cdot \text{L}^{-1} = \text{mg} \cdot \text{mL}^{-1}$]. X is the type of sample—isolated
815 mitochondria, tissue homogenate, permeabilized muscle fibers or cells (**Table 4**). m_{ce} [mg] is the total
816 mass of all cells in an instrumental chamber, whereas $m_{Nce} = m_{ce} \cdot N_{ce}^{-1}$ [$\text{mg} \cdot \text{x}^{-1}$] is the (average) mass of
817 an individual cell (**Table 5**).

818
819

820 **4.2.2. Size-specific flux:** Cellular O_2 flow can be compared between cells of identical size. To take
821 into account changes and differences in cell size (Renner *et al* 2003), normalization is required to
822 obtain cell size-specific or mitochondrial marker-specific O_2 flux (**Figure 5**).

823

824 • **Mass-specific flux, $J_{\text{O}_2/mX}$** [$\text{mol} \cdot \text{s}^{-1} \cdot \text{kg}^{-1}$]: Mass-specific flux is the expression of respiration per
825 mass of sample, m_X [mg]. Chamber volume-specific flux, J_{V,O_2} , is divided by mass concentration
826 of X in the chamber, $J_{\text{O}_2/mX} = J_{V,\text{O}_2} \cdot C_{mX}^{-1}$. Cell mass-specific flux is obtained by dividing flow per
827 cell by mass per cell, $J_{\text{O}_2/mce} = I_{\text{O}_2/Nce} \cdot m_{Nce}^{-1}$.

828 • **Cell volume-specific flux, $J_{\text{O}_2/VX}$** [$\text{mol} \cdot \text{s}^{-1} \cdot \text{m}^{-3}$]: Sample volume-specific flux is obtained by
829 expressing respiration per volume of sample.

830

831 If size-specific O_2 flux is constant and independent of sample size, then there is no interaction
832 between the subsystems. For example, 1.5 mg and 3.0 mg sub-samples of muscle tissue respire at
833 identical mass-specific flux. If mass-specific O_2 flux, however, changes as a function of the mass of
834 a tissue sample, cells or isolated mitochondria in the instrumental chamber, then the nature of the
835 interaction becomes an issue. Therefore, cell concentration must be optimized, particularly in
836 experiments carried out in wells, considering the confluency of the cell monolayer or clumps of
837 cells (Salabei *et al* 2014).

838 The complexity changes when considering the scaling law of respiratory physiology. Strong
839 interactions are revealed between O_2 flow and body mass of an individual organism: *basal*
840 metabolic rate (flow) does not increase linearly with body mass, whereas *maximum* mass-specific
841 O_2 flux, $\dot{V}_{\text{O}_2\text{max}}$ or $\dot{V}_{\text{O}_2\text{peak}}$, is approximately constant across a large range of individual body mass
842 (Weibel and Hoppeler 2005). Individuals, breeds and species, however, deviate substantially from
843 this relationship. $\dot{V}_{\text{O}_2\text{peak}}$ of human endurance athletes is 60 to 80 $\text{mL O}_2 \cdot \text{min}^{-1} \cdot \text{kg}^{-1}$ body mass,
844 converted to $J_{\text{O}_2\text{peak}/m\text{Norg}}$ of 45 to 60 $\text{nmol} \cdot \text{s}^{-1} \cdot \text{g}^{-1}$ (Gnaiger 2020; **Table 6**).

845

846 **4.3. Marker-specific flux: per mitochondrial content**

847

848 Tissues can contain multiple cell populations that may have distinct mitochondrial subtypes.
849 Mitochondria undergo dynamic fission and fusion cycles, and can exist in multiple stages and sizes
850 that may be altered by a range of factors. The isolation of mitochondria (often achieved through
851 differential centrifugation) can therefore yield a subsample of the mitochondrial types present in
852 a tissue, depending on the isolation protocols utilized. This possible bias should be taken into
853 account when planning experiments using isolated mitochondria. Different sizes of mitochondria
854 are enriched at specific centrifugation speeds, which can be used strategically for isolation of
855 mitochondrial subpopulations.

856 Part of the mitochondrial content of a tissue is lost during preparation of isolated
857 mitochondria. The fraction of isolated mitochondria obtained from a tissue sample is expressed
858 as mitochondrial recovery. At a high mitochondrial recovery, the fraction of isolated mitochondria
859 is more representative of the total mitochondrial population than in preparations characterized
860 by low recovery. Determination of the mitochondrial recovery and yield is based on measurement
861 of the concentration of a mitochondrial marker in the stock suspension of isolated mitochondria,
862 $C_{mtE,\text{stock}}$ and crude tissue homogenate, $C_{mtE,\text{thom}}$, which together provide information on the specific
863 mitochondrial density in the sample, D_{mtE} (**Table 4**).

864 When discussing concepts of normalization, it is essential to consider the question posed by
865 the study. If the study aims at comparing tissue performance—such as the effects of a treatment
866 on a specific tissue, then normalization for tissue mass or protein content is appropriate. However,

867 if the aim is to find differences in mitochondrial function independent of mitochondrial density
 868 (**Table 4**), then normalization to a mitochondrial marker is imperative (**Figure 5**). One cannot
 869 assume that quantitative changes in various markers—such as mitochondrial proteins—
 870 necessarily occur in parallel with one another. It should be established that the marker chosen is
 871 not selectively altered by the performed treatment. In conclusion, the normalization must reflect
 872 the question under investigation to reach a satisfying answer. On the other hand, the goal of
 873 comparing results across projects and institutions requires standardization on normalization for
 874 entry into a databank.

875

876 **4.3.1. Mitochondrial concentration, C_{mtE} , and mitochondrial markers:** Mitochondrial
 877 organelles compose a dynamic cellular reticulum in various states of fusion and fission. Hence, the
 878 definition of an ‘amount’ of mitochondria is often misconceived: mitochondria cannot be counted
 879 reliably as a number of occurring elementary components. Therefore, quantification of the
 880 amount of mitochondria depends on the measurement of chosen mitochondrial markers.
 881 ‘Mitochondria are the structural and functional elementary units of cell respiration’ (Gnaiger 2020).
 882 The quantity of a mitochondrial marker can reflect the amount of mitochondrial elementary
 883 components, mtE , expressed in various mitochondrial elementary units [mtEU] specific for each
 884 measured mt-marker (**Table 4**). However, since mitochondrial quality may change in response to
 885 stimuli—particularly in mitochondrial dysfunction (Campos *et al* 2017) and after exercise
 886 training (Pesta *et al* 2011) and during aging (Daum *et al* 2013)—some markers can vary while
 887 others are unchanged: (1) Mitochondrial volume and membrane area are structural markers,
 888 whereas mitochondrial protein mass is commonly used as a marker for isolated mitochondria. (2)
 889 Molecular and enzymatic mitochondrial markers (amounts or activities) can be selected as matrix
 890 markers, *e.g.*, citrate synthase activity, mtDNA; mtIM-markers, *e.g.*, cytochrome *c* oxidase activity,
 891 aa_3 content, cardiolipin, or mtOM-markers, *e.g.*, the voltage-dependent anion channel (VDAC),
 892 TOM20. (3) Extending the measurement of mitochondrial marker enzyme activity to
 893 mitochondrial pathway capacity, ET- or OXPHOS-capacity can be considered as an integrative
 894 functional mitochondrial marker.

895 Depending on the type of mitochondrial marker, the mitochondrial elementary entity, mtE , is
 896 expressed in marker-specific units. Mitochondrial concentration in the instrumental chamber and
 897 mitochondrial density in the tissue of origin are quantified as (1) a quantity for normalization in
 898 functional analyses, C_{mtE} , and (2) a physiological output that is the result of mitochondrial
 899 biogenesis and degradation, D_{mtE} , respectively (**Table 4**). It is recommended, therefore, to
 900 distinguish *experimental mitochondrial concentration*, $C_{mtE} = mtE \cdot V^{-1}$ and *physiological*
 901 *mitochondrial density*, $D_{mtE} = mtE \cdot m_X^{-1}$. Then mitochondrial density is the amount of mitochondrial
 902 elementary components per mass of tissue, which is a biological variable (**Figure 5**). The
 903 experimental variable is mitochondrial density multiplied by sample mass concentration in the
 904 measuring chamber, $C_{mtE} = D_{mtE} \cdot C_{mX}$, or mitochondrial content multiplied by sample number
 905 concentration, $C_{mtE} = mtE_X \cdot C_{NX}$ (**Table 4**).

906

907 **4.3.2. mt-Marker-specific flux, $J_{O_2/mtE}$:** Volume-specific metabolic O_2 flux depends on: (1) the
 908 sample concentration in the volume of the instrumental chamber, C_{mX} , or C_{NX} ; (2) the
 909 mitochondrial density in the sample, $D_{mtE} = mtE \cdot m_X^{-1}$ or $mtE_X = mtE \cdot N_X^{-1}$; and (3) the specific
 910 mitochondrial activity or performance per mitochondrial elementary marker, $J_{O_2/mtE} = J_{V,O_2} \cdot C_{mtE}^{-1}$
 911 [$\text{mol} \cdot \text{s}^{-1} \cdot \text{mtEU}^{-1}$] (**Table 4**). Obviously, the numerical results for $J_{O_2/mtE}$ vary with the type of
 912 mitochondrial marker chosen for measurement of mtE and $C_{mtE} = mtE \cdot V^{-1}$ [$\text{mtEU} \cdot \text{m}^{-3}$].

913

914 **Reference to Part 3. Quantitative mitochondrial physiology. Mitochondrial markers**

915 Different methods for the quantification of mitochondrial markers have different strengths and
 916 weaknesses. Some problems are common for all mitochondrial markers, mtE : (1) Accuracy of
 917 measurement is crucial, since even a highly accurate and reproducible measurement of chamber
 918 volume-specific O_2 flux results in an inaccurate and noisy expression if normalized by a biased
 919 and noisy measurement of a mitochondrial marker. This problem is acute in mitochondrial
 920 respiration because the denominators used (the mitochondrial markers) are often small moieties

921 of which accurate and precise determination is difficult. In contrast, an *internal* marker is used
922 when O₂ fluxes measured in substrate-uncoupler-inhibitor titration protocols are normalized for
923 flux in a defined respiratory reference state within the assay, which yields flux control ratios, *FCRs*.
924 *FCRs* are independent of externally measured markers and, therefore, are statistically robust,
925 considering the limitations of ratios in general (Jasienski and Bazzaz 1999). *FCRs* indicate
926 qualitative changes of mitochondrial respiratory control, with highest quantitative resolution,
927 separating the effect of mitochondrial density on $J_{O_2/mx}$ and $I_{O_2/Nx}$ from that of function per
928 mitochondrial elementary marker, $J_{O_2/mtE}$ (Pesta *et al* 2011; Gnaiger 2020). (2) If mitochondrial
929 quality does not change and only the amount of mitochondria varies as a determinant of mass-
930 specific flux, any marker is equally qualified in principle; then in practice selection of the optimum
931 marker depends only on the accuracy and precision of measurement of the mitochondrial marker.
932 (3) If mitochondrial flux control ratios change, then there may not be any best mitochondrial
933 marker. In general, measurement of multiple mitochondrial markers enables a comparison and
934 evaluation of normalization for these mitochondrial markers. Particularly during postnatal
935 development, the activity of marker enzymes—such as cytochrome *c* oxidase and citrate
936 synthase—follows different time courses (Drahota *et al* 2004). Evaluation of mitochondrial
937 markers in healthy controls is insufficient for providing guidelines for application in the diagnosis
938 of pathological states and specific treatments.

939 In line with the concept of the respiratory control ratio (Chance and Williams 1955a), the most
940 readily used normalization is that of flux control ratios and flux control factors (Gnaiger 2020).
941 Selection of the state of maximum flux in a protocol as the reference state has the advantages of:
942 (1) internal normalization; (2) statistically validated linearization of the response in the range of
943 0 to 1; and (3) consideration of maximum flux for integrating a large number of elementary steps
944 in the OXPHOS- or ET-pathways. This reduces the risk of selecting a functional marker that is
945 specifically altered by the treatment or pathology, yet increases the chance that the highly
946 integrative pathway is disproportionately affected, *e.g.*, the OXPHOS- rather than ET-pathway in
947 case of an enzymatic defect in the phosphorylation-pathway. In this case, additional information
948 can be obtained by reporting flux control ratios based on a reference state that indicates stable
949 tissue-mass specific flux.

950 Stereological measurement of mitochondrial content via two-dimensional transmission
951 electron microscopy is considered as the gold standard in determination of mitochondrial volume
952 fractions in cells and tissues (Weibel, Hoppeler, 2005). Accurate determination of three-
953 dimensional volume by two-dimensional microscopy, however, is both time consuming and
954 statistically challenging (Larsen *et al* 2012). The validity of using mitochondrial marker enzymes
955 (citrate synthase activity, CI to CIV amount or activity) for normalization of flux is limited in part
956 by the same factors that apply to flux control ratios. Strong correlations between various
957 mitochondrial markers and citrate synthase activity (Reichmann *et al* 1985; Boushel *et al* 2007;
958 Mogensen *et al* 2007) are expected in a specific tissue of healthy persons and in disease states not
959 specifically targeting citrate synthase. Citrate synthase activity is acutely modifiable by exercise
960 (Tonkonogi *et al* 1997; Leek *et al* 2001). Evaluation of mitochondrial markers related to a selected
961 age and sex cohort cannot be extrapolated to provide recommendations for normalization in
962 respirometric diagnosis of disease, in different states of development and aging, different cell
963 types, tissues, and species. mtDNA normalized to nDNA via qPCR is correlated to functional
964 mitochondrial markers including OXPHOS- and ET-capacity in some cases (Puntschart *et al* 1995;
965 Wang *et al* 1999; Menshikova *et al* 2006; Boushel *et al* 2007; Ehinger *et al* 2015), but lack of such
966 correlations have been reported (Menshikova *et al* 2005; Schultz and Wiesner 2000; Pesta *et al*
967 2011). Several studies indicate a strong correlation between cardiolipin content and increase in
968 mitochondrial function with exercise (Menshikova *et al* 2005; Menshikova *et al* 2007; Larsen *et al*
969 2012; Faber *et al* 2014), but it has not been evaluated as a general mitochondrial biomarker in
970 disease. With no single best mitochondrial marker, a good strategy is to quantify several different
971 biomarkers to minimize the decorrelating effects caused by diseases, treatments, or other factors.
972 Determination of multiple markers, particularly a matrix marker and a marker from the mtIM,
973 allows tracking changes in mitochondrial quality defined by their ratio.

974

975 5. Normalization of rate per system

976

977 5.1. Flow: per chamber

978

979 The instrumental system (chamber) is part of the measurement instrument, separated from the
 980 environment as an isolated, closed, open, isothermal or non-isothermal system (**Table 4**).
 981 Reporting O₂ flows per respiratory chamber, I_{O_2} [nmol·s⁻¹], restricts the analysis to intra-
 982 experimental comparison of relative differences.

983

984 5.2. Flux: per chamber volume

985

986 **5.2.1. System-specific flux, J_{V,O_2} :** We distinguish between (1) the *system* with volume V and mass
 987 m defined by the system boundaries, and (2) the *sample* or *objects* with volume V_X and mass m_X
 988 that are enclosed in the instrumental chamber (**Figure 5**). Metabolic O₂ flow per object, I_{O_2/m_X} , is
 989 the total O₂ flow in the system divided by the number of objects, N_X , in the system. I_{O_2/m_X} increases
 990 as the mass of the object is increased. Sample mass-specific O₂ flux, J_{O_2/m_X} should be independent
 991 of the mass-concentration of the subsample obtained from the same tissue or cell culture, but
 992 system volume-specific O₂ flux, J_{V,O_2} (per liquid volume of the instrumental chamber), increases in
 993 proportion to the mass of the sample in the chamber. Although J_{V,O_2} depends on mass-
 994 concentration of the sample in the chamber, it should be independent of the chamber (system)
 995 volume at constant sample mass-concentration. There are practical limitations to increasing the
 996 mass-concentration of the sample in the chamber, when one is concerned about crowding effects
 997 and instrumental time resolution. The wall of the chamber and the enclosed solid stirrer are not
 998 counted as part of the chamber volume.

999

1000 **5.2.2. Advancement per volume:** When the reactor volume does not change during the reaction,
 1001 which is typical for liquid phase reactions, the volume-specific *flux of a chemical reaction* r is the
 1002 time derivative of the advancement of the reaction per unit volume, $J_{V,rB} = d_r \xi_B / dt \cdot V^{-1}$ [(mol·s⁻¹)·L⁻¹].
 1003 The *rate of concentration change* is dc_B / dt [(mol·L⁻¹)·s⁻¹], where concentration is $c_B = n_B \cdot V^{-1}$. There
 1004 is a difference between (1) J_{V,rO_2} [mol·s⁻¹·L⁻¹] and (2) rate of concentration change [mol·L⁻¹·s⁻¹].
 1005 These merge into a single expression only in closed systems. In open systems, internal
 1006 transformations (catabolic flux, O₂ consumption) are distinguished from external flux (such as O₂
 1007 supply). External fluxes of all substances are zero in closed systems. In a closed chamber O₂
 1008 consumption (internal flux of catabolic reactions k ; I_{kO_2} [pmol·s⁻¹]) causes a decline in the amount
 1009 of O₂ in the system, n_{O_2} [nmol]. Normalization of these quantities for the volume of the system, V
 1010 [L \equiv dm³], yields volume-specific O₂ flux, $J_{V,kO_2} = I_{kO_2} / V$ [nmol·s⁻¹·L⁻¹], and O₂ concentration, [O₂] or
 1011 $c_{O_2} = n_{O_2} \cdot V^{-1}$ [μ mol·L⁻¹ = μ M = nmol·mL⁻¹]. Instrumental background O₂ flux is due to external flux
 1012 into a non-ideal closed respirometer, so total volume-specific flux has to be corrected for
 1013 instrumental background O₂ flux—O₂ diffusion into or out of the instrumental chamber. J_{V,kO_2} is
 1014 relevant mainly for methodological reasons and should be compared with the accuracy of
 1015 instrumental resolution of background-corrected flux, *e.g.*, ± 1 nmol·s⁻¹·L⁻¹ (Gnaiger 2001).
 1016 ‘Catabolic’ indicates O₂ flux, J_{kO_2} , corrected for: (1) instrumental background O₂ flux; (2) chemical
 1017 background O₂ flux due to autoxidation of chemical components added to the incubation medium;
 1018 and (3) *Rox* for O₂-consuming side reactions unrelated to the catabolic pathway k .

1019

1020 6. Conversion of units

1021

1022 Many different units have been used to report the O₂ consumption rate, OCR (**Table 6**). SI base
 1023 units provide the common reference to introduce the theoretical principles (**Figure 5**), and are
 1024 used with appropriately chosen SI prefixes to express numerical data in the most practical format,
 1025 with an effort towards unification within specific areas of application (**Table 7**). Reporting data

1026 in SI units—including the mole [mol], coulomb [C], joule [J], and second [s]—should be
1027 encouraged, particularly by journals that propose the use of SI units.

1028 Although volume is expressed as m^3 using the SI base unit, the litre [dm^3] is a conventional unit
1029 of volume for concentration and is used for most solution chemical kinetics. If one multiplies $I_{\text{O}_2/N_{\text{ce}}}$
1030 by $C_{N_{\text{ce}}}$, then the result will not only be the amount of O_2 [mol] consumed per time [s^{-1}] in one litre
1031 [L^{-1}], but also the change in O_2 concentration per second (for any volume of an ideally closed
1032 system). This is ideal for kinetic modeling as it blends with chemical rate equations where
1033 concentrations are typically expressed in $\text{mol}\cdot\text{L}^{-1}$ (Wagner *et al* 2011). In studies of multinuclear
1034 cells—such as differentiated skeletal muscle cells—it is easy to determine the number of nuclei
1035 but not the total number of cells. A generalized concept, therefore, is obtained by substituting cells
1036 by nuclei as the sample entity. This does not hold, however, for non-nucleated platelets.

1037 For studies of cells, we recommend that respiration be expressed, as far as possible, as: (1) O_2
1038 flux normalized for a mitochondrial marker, for separation of the effects of mitochondrial quality
1039 and content on cell respiration (this includes *FCRs* as a normalization for a functional
1040 mitochondrial marker); (2) O_2 flux in units of cell volume or mass, for comparison of respiration
1041 of cells with different cell size (Renner *et al* 2003) and with studies on tissue preparations, and
1042 (3) O_2 flow in units of attomole (10^{-18} mol) of O_2 consumed per second by each cell [$\text{amol}\cdot\text{s}^{-1}\cdot\text{cell}^{-1}$],
1043 numerically equivalent to [$\text{pmol}\cdot\text{s}^{-1}\cdot 10^{-6}$ cells]. This convention allows information to be easily
1044 used when designing experiments in which O_2 flow must be considered. For example, to estimate
1045 the volume-specific O_2 flux in an instrumental chamber that would be expected at a particular cell
1046 number concentration, one simply needs to multiply the flow per cell by the number of cells per
1047 volume of interest. This provides the amount of O_2 [mol] consumed per time [s^{-1}] per unit volume
1048 [L^{-1}]. At an O_2 flow of $100 \text{ amol}\cdot\text{s}^{-1}\cdot\text{cell}^{-1}$ and a cell concentration of $10^9 \text{ cells}\cdot\text{L}^{-1}$ ($10^6 \text{ cells}\cdot\text{mL}^{-1}$), the
1049 volume-specific O_2 flux is $100 \text{ nmol}\cdot\text{s}^{-1}\cdot\text{L}^{-1}$ ($100 \text{ pmol}\cdot\text{s}^{-1}\cdot\text{mL}^{-1}$).

1050 ET-capacity in human cell types including HEK 293, primary HUVEC, and fibroblasts ranges
1051 from 50 to $180 \text{ amol}\cdot\text{s}^{-1}\cdot\text{cell}^{-1}$, measured in living cells in the noncoupled state (Gnaiger 2020). At
1052 $100 \text{ amol}\cdot\text{s}^{-1}\cdot\text{cell}^{-1}$ corrected for *Rox*, the current across the mt- membranes, I_{H^+e} , approximates
1053 $193 \text{ pA}\cdot\text{cell}^{-1}$ or 0.2 nA per cell. See Rich (2003) for an extension of quantitative bioenergetics from
1054 the molecular to the human scale, with a transmembrane proton flux equivalent to 520 A in an
1055 adult at a catabolic power of -110 W. Modelling approaches illustrate the link between
1056 protonmotive force and currents (Willis *et al* 2016).

1057 We consider isolated mitochondria as powerhouses and proton pumps as molecular machines
1058 to relate experimental results to energy metabolism of living cells. The cellular $\text{P}\gg/\text{O}_2$ based on
1059 oxidation of glycogen is increased by the glycolytic (fermentative) substrate-level
1060 phosphorylation of 3 $\text{P}\gg/\text{Glyc}$ or 0.5 mol $\text{P}\gg$ for each mol O_2 consumed in the complete oxidation
1061 of a mol glycosyl unit (Glyc). Adding 0.5 to the mitochondrial $\text{P}\gg/\text{O}_2$ ratio of 5.4 yields a
1062 bioenergetic cell physiological $\text{P}\gg/\text{O}_2$ ratio close to 6. Two NADH equivalents are formed during
1063 glycolysis and transported from the cytosol into the mitochondrial matrix, either by the malate-
1064 aspartate shuttle or by the glycerophosphate shuttle (Figure 1a) resulting in different theoretical
1065 yields of ATP generated by mitochondria, the energetic cost of which potentially must be taken
1066 into account. Considering also substrate-level phosphorylation in the TCA cycle, this high $\text{P}\gg/\text{O}_2$
1067 ratio not only reflects proton translocation and OXPHOS studied in isolation, but integrates
1068 mitochondrial physiology with energy transformation in the living cell (Gnaiger 1993a).

1069

1070 7. Conclusions

1071

1072 Catabolic cell respiration is the process of exergonic and exothermic energy transformation in
1073 which scalar redox reactions are coupled to vectorial ion translocation across a semipermeable
1074 membrane, which separates the small volume of a bacterial cell or mitochondrion from the larger
1075 volume of its surroundings. The electrochemical exergy can be partially conserved in the
1076 phosphorylation of ADP to ATP or in ion pumping, or dissipated in an electrochemical short-
1077 circuit. Respiration is thus clearly distinguished from fermentation as the counterparts of cellular
1078 core energy metabolism. An O_2 flux balance scheme illustrates the relationships and general
1079 definitions (Figures 1 and 2).

1080

1081

Box 2: Recommendations for studies with mitochondrial preparations

1082

1083

- Normalization of respiratory rates should be provided as far as possible:

1084

A. Sample normalization

1086 1. *Object-specific biophysical normalization*: on a per organism or per cell basis as O₂ flow; this1087 may not be possible when dealing with coenocytic organisms, *e.g.*, filamentous fungi, or tissues1088 without cross-walls separating individual cells, *e.g.*, muscle fibers.1089 2. *Size-specific cellular normalization*: per g protein; per organism-, cell- or tissue-mass as mass-1090 specific O₂ flux; per cell volume as cell volume-specific flux.1091 3. *Mitochondrial normalization*: per mitochondrial marker as mt-specific flux.

B. Chamber normalization

1094 1. Chamber volume-specific flux, J_V [pmol·s⁻¹·mL⁻¹], is reported for quality control in relation to

1095 instrumental sensitivity and limit of detection of volume-specific flux.

1096 2. Sample concentration in the instrumental chamber is reported as number concentration, mass

1097 concentration, or mitochondrial concentration; this is a component of the measuring

1098 conditions. With information on cell size and the use of multiple normalizations, maximum

1099 potential information is available (Renner *et al* 2003; Wagner *et al* 2011; Gnaiger 2020).1100 Reporting flow in a respiratory chamber [nmol·s⁻¹] is discouraged, since it restricts the analysis

1101 to intra-experimental comparison of relative (qualitative) differences.

- Catabolic mitochondrial respiration is distinguished from residual O₂ consumption. Fluxes in

1103 mitochondrial coupling states should be, as far as possible, corrected for residual O₂

1104 consumption.

- Different mechanisms of uncoupling should be distinguished by defined terms. The tightness

1106 of coupling relates to these uncoupling mechanisms, whereas the coupling stoichiometry

1107 varies as a function the substrate type involved in ET-pathways with either three or two redox

1108 proton pumps operating in series. Separation of tightness of coupling from the pathway-

1109 dependent coupling stoichiometry is possible only when the substrate type undergoing

1110 oxidation remains the same for respiration in LEAK-, OXPHOS-, and ET-states. In studies of the

1111 tightness of coupling, therefore, simple substrate-inhibitor combinations should be applied to

1112 exclude a shift in substrate competition that may occur when providing physiological substrate

1113 cocktails.

- In studies of isolated mitochondria, the mitochondrial recovery and yield should be reported.

1115 Experimental criteria such as transmission electron microscopy for evaluation of purity versus

1116 integrity should be considered. Mitochondrial markers—such as citrate synthase activity as an

1117 enzymatic matrix marker—provide a link to the tissue of origin on the basis of calculating the

1118 mitochondrial recovery, *i.e.*, the fraction of mitochondrial marker obtained from a unit mass of

1119 tissue. Total mitochondrial protein is frequently applied as a mitochondrial marker, which is

1120 restricted to isolated mitochondria.

- In studies of permeabilized cells, the viability of the cell culture or cell suspension of origin

1122 should be reported. Normalization should be evaluated for total cell count or viable cell count.

- Terms and symbols are summarized in **Table 8**. Their use will facilitate transdisciplinary

1124 communication and support further development of a consistent theory of bioenergetics and

1125 mitochondrial physiology. Technical terms related to and defined with normal words can be

1126 used as index terms in data repositories, support the creation of ontologies towards semantic

1127 information processing (MitoPedia), and help in communicating analytical findings as

1128 impactful data-driven stories. *'Making data available without making it understandable may be*1129 *worse than not making it available at all'* (National Academies of Sciences, Engineering, and

1130 Medicine 2018). Success will depend on taking further steps: (1) exhaustive text-mining

1131 considering Omics data and functional data; (2) network analysis of Omics data with

1132 bioinformatics tools; (3) cross-validation with distinct bioinformatics approaches; (4)

1133 correlation with physiological data; (5) guidelines for biological validation of network data.

1134 This is a call to carefully contribute to FAIR principles (Findable, Accessible, Interoperable,
1135 Reusable) for the sharing of scientific data.

1136
1137 Experimentally, respiration is separated in mitochondrial preparations from the interactions
1138 with the fermentative pathways of the living cell. OXPHOS analysis is based on the study of
1139 mitochondrial preparations complementary to bioenergetic investigations of (1)
1140 submitochondrial particles and molecular structures, (2) living cells, and (3) organisms—from
1141 model organisms to the human species including healthy and diseased persons (patients).
1142 Different mechanisms of respiratory uncoupling have to be distinguished (Figure 3). Metabolic
1143 fluxes measured in defined coupling and pathway control states (Figures 5 and 6) provide
1144 insights into the meaning of cellular and organismic respiration.

1145 The optimal choice for expressing mitochondrial and cell respiration as O₂ flow per biological
1146 sample, and normalization for specific tissue-markers (volume, mass, protein) and mitochondrial
1147 markers (volume, protein, content, mtDNA, activity of marker enzymes, respiratory reference
1148 state) is guided by the scientific question under study. Interpretation of the data depends critically
1149 on appropriate normalization (Figure 5).

1150 MitoEAGLE can serve as a gateway to better diagnose mitochondrial respiratory adaptations
1151 and defects linked to genetic variation, age-related health risks, sex-specific mitochondrial
1152 performance, lifestyle with its effects on degenerative diseases, and thermal and chemical
1153 environment. The present recommendations on coupling control states and rates are focused on
1154 studies using mitochondrial preparations (Box 2). These will be extended in a series of reports on
1155 pathway control of mitochondrial respiration, respiratory states and rates in living cells,
1156 respiratory flux control ratios, and harmonization of experimental procedures.

1157 1158 References

- 1159
1160 Altmann R (1894) Die Elementarorganismen und ihre Beziehungen zu den Zellen. Zweite vermehrte
1161 Auflage. Verlag Von Veit & Comp, Leipzig:160 pp.
- 1162 Baggeto LG, Testa-Perussini R (1990) Role of acetoin on the regulation of intermediate metabolism of
1163 Ehrlich ascites tumor mitochondria: its contribution to membrane cholesterol enrichment modifying
1164 passive proton permeability. Arch Biochem Biophys 283:341-8.
- 1165 Beard DA (2005) A biophysical model of the mitochondrial respiratory system and oxidative
1166 phosphorylation. PLoS Comput Biol 1(4):e36.
- 1167 Benda C (1898) Weitere Mitteilungen über die Mitochondria. Verh Dtsch Physiol Ges:376-83.
- 1168 Birkedal R, Laasmaa M, Vendelin M (2014) The location of energetic compartments affects energetic
1169 communication in cardiomyocytes. Front Physiol 5:376.
- 1170 Blier PU, Dufresne F, Burton RS (2001) Natural selection and the evolution of mtDNA-encoded peptides:
1171 evidence for intergenomic co-adaptation. Trends Genet 17:400-6.
- 1172 Blier PU, Guderley HE (1993) Mitochondrial activity in rainbow trout red muscle: the effect of temperature
1173 on the ADP-dependence of ATP synthesis. J Exp Biol 176:145-58.
- 1174 Breton S, Beaupré HD, Stewart DT, Hoeh WR, Blier PU (2007) The unusual system of doubly uniparental
1175 inheritance of mtDNA: isn't one enough? Trends Genet 23:465-74.
- 1176 Brown GC (1992) Control of respiration and ATP synthesis in mammalian mitochondria and cells. Biochem
1177 J 284:1-13.
- 1178 Burger G, Gray MW, Forget L, Lang BF (2013) Strikingly bacteria-like and gene-rich mitochondrial genomes
1179 throughout jakobid protists. Genome Biol Evol 5:418-38.
- 1180 Calvo SE, Klausner CR, Mootha VK (2016) MitoCarta2.0: an updated inventory of mammalian mitochondrial
1181 proteins. Nucleic Acids Research 44:D1251-7.
- 1182 Calvo SE, Julien O, Clauser KR, Shen H, Kamer KJ, Wells JA, Mootha VK (2017) Comparative analysis of
1183 mitochondrial N-termini from mouse, human, and yeast. Mol Cell Proteomics 16:512-23.
- 1184 Campos JC, Queliconi BB, Bozi LHM, Bechara LRG, Dourado PMM, Andres AM, Jannig PR, Gomes KMS,
1185 Zambelli VO, Rocha-Resende C, Guatimosim S, Brum PC, Mochly-Rosen D, Gottlieb RA, Kowaltowski AJ,
1186 Ferreira JCB (2017) Exercise reestablishes autophagic flux and mitochondrial quality control in heart
1187 failure. Autophagy 13:1304-317.
- 1188 Canton M, Luvisetto S, Schmehl I, Azzone GF (1995) The nature of mitochondrial respiration and
1189 discrimination between membrane and pump properties. Biochem J 310:477-81.

- 1190 Carrico C, Meyer JG, He W, Gibson BW, Verdin E (2018) The mitochondrial acylome emerges: proteomics,
1191 regulation by Sirtuins, and metabolic and disease implications. *Cell Metab* 27:497-512.
- 1192 Chan DC (2006) Mitochondria: dynamic organelles in disease, aging, and development. *Cell* 125:1241-52.
- 1193 Chance B, Williams GR (1955a) Respiratory enzymes in oxidative phosphorylation. I. Kinetics of oxygen
1194 utilization. *J Biol Chem* 217:383-93.
- 1195 Chance B, Williams GR (1955b) Respiratory enzymes in oxidative phosphorylation: III. The steady state. *J*
1196 *Biol Chem* 217:409-27.
- 1197 Chance B, Williams GR (1955c) Respiratory enzymes in oxidative phosphorylation. IV. The respiratory
1198 chain. *J Biol Chem* 217:429-38.
- 1199 Chance B, Williams GR (1956) The respiratory chain and oxidative phosphorylation. *Adv Enzymol Relat*
1200 *Subj Biochem* 17:65-134.
- 1201 Chowdhury SK, Djordjevic J, Albensi B, Fernyhough P (2015) Simultaneous evaluation of substrate-
1202 dependent oxygen consumption rates and mitochondrial membrane potential by TMRM and safranin in
1203 cortical mitochondria. *Biosci Rep* 36:e00286.
- 1204 Cobb LJ, Lee C, Xiao J, Yen K, Wong RG, Nakamura HK, Mehta HH, Gao Q, Ashur C, Huffman DM, Wan J,
1205 Muzumdar R, Barzilay N, Cohen P (2016) Naturally occurring mitochondrial-derived peptides are age-
1206 dependent regulators of apoptosis, insulin sensitivity, and inflammatory markers. *Aging (Albany NY)*
1207 8:796-809.
- 1208 Cohen ER, Cvitas T, Frey JG, Holmström B, Kuchitsu K, Marquardt R, Mills I, Pavese F, Quack M, Stohner J,
1209 Strauss HL, Takami M, Thor HL (2008) Quantities, units and symbols in physical chemistry, IUPAC Green
1210 Book, 3rd Edition, 2nd Printing, IUPAC & RSC Publishing, Cambridge.
- 1211 Cooper H, Hedges LV, Valentine JC, eds (2009) The handbook of research synthesis and meta-analysis.
1212 Russell Sage Foundation.
- 1213 Coopersmith J (2010) Energy, the subtle concept. The discovery of Feynman's blocks from Leibnitz to
1214 Einstein. Oxford University Press:400 pp.
- 1215 Cummins J (1998) Mitochondrial DNA in mammalian reproduction. *Rev Reprod* 3:172-82.
- 1216 Dai Q, Shah AA, Garde RV, Yonish BA, Zhang L, Medvitz NA, Miller SE, Hansen EL, Dunn CN, Price TM (2013)
1217 A truncated progesterone receptor (PR-M) localizes to the mitochondrion and controls cellular
1218 respiration. *Mol Endocrinol* 27:741-53.
- 1219 Daum B, Walter A, Horst A, Osiewacz HD, Kühlbrandt W (2013) Age-dependent dissociation of ATP synthase
1220 dimers and loss of inner-membrane cristae in mitochondria. *Proc Natl Acad Sci U S A* 110:15301-6.
- 1221 Diebold LP, Gil HJ, Gao P, Martinez CA, Weinberg SE, Chandel NS (2019) Mitochondrial Complex III is
1222 necessary for endothelial cell proliferation during angiogenesis. *Nat Metab* 1:158-71.
- 1223 Divakaruni AS, Brand MD (2011) The regulation and physiology of mitochondrial proton leak. *Physiology*
1224 (Bethesda) 26:192-205.
- 1225 Doerrier C, Garcia-Souza LF, Krumschnabel G, Wohlfarter Y, Mészáros AT, Gnaiger E (2018) High-Resolution
1226 FluoRespirometry and OXPHOS protocols for human cells, permeabilized fibres from small biopsies of
1227 muscle, and isolated mitochondria. *Methods Mol Biol* 1782 (Palmeira CM, Moreno AJ, eds):
1228 Mitochondrial Bioenergetics, 978-1-4939-7830-4.
- 1229 Doskey CM, van 't Erve TJ, Wagner BA, Buettner GR (2015) Moles of a substance per cell is a highly
1230 informative dosing metric in cell culture. *PLoS One* 10:e0132572.
- 1231 Drahotová Z, Milerová M, Stieglerová A, Houstek J, Ostádal B (2004) Developmental changes of cytochrome *c*
1232 oxidase and citrate synthase in rat heart homogenate. *Physiol Res* 53:119-22.
- 1233 Duarte FV, Palmeira CM, Rolo AP (2014) The role of microRNAs in mitochondria: small players acting wide.
1234 *Genes (Basel)* 5:865-86.
- 1235 Ehinger JK, Morota S, Hansson MJ, Paul G, Elmer E (2015) Mitochondrial dysfunction in blood cells from
1236 amyotrophic lateral sclerosis patients. *J Neurol* 262:1493-503.
- 1237 Ehinger JK, Piel S, Ford R, Karlsson M, Sjövall F, Frostner EÅ, Morota S, Taylor RW, Turnbull DM, Cornell C,
1238 Moss SJ, Metzsch C, Hansson MJ, Fliri H, Elmer E (2016) Cell-permeable succinate prodrugs bypass
1239 mitochondrial complex I deficiency. *Nat Commun* 7:12317.
- 1240 Ernster L, Schatz G (1981) Mitochondria: a historical review. *J Cell Biol* 91:227s-55s.
- 1241 Estabrook RW (1967) Mitochondrial respiratory control and the polarographic measurement of ADP:O
1242 ratios. *Methods Enzymol* 10:41-7.
- 1243 Faber C, Zhu ZJ, Castellino S, Wagner DS, Brown RH, Peterson RA, Gates L, Barton J, Bickett M, Hagerty L,
1244 Kimbrough C, Sola M, Bailey D, Jordan H, Elangbam CS (2014) Cardiolipin profiles as a potential
1245 biomarker of mitochondrial health in diet-induced obese mice subjected to exercise, diet-restriction and
1246 ephedrine treatment. *J Appl Toxicol* 34:1122-9.
- 1247 Feagin JE, Harrell MI, Lee JC, Coe KJ, Sands BH, Cannone JJ, Tami G, Schnare MN, Gutell RR (2012) The
1248 fragmented mitochondrial ribosomal RNAs of *Plasmodium falciparum*. *PLoS One* 7:e38320.
- 1249 Fell D (1997) Understanding the control of metabolism. Portland Press.

- 1250 Forstner H, Gnaiger E (1983) Calculation of equilibrium oxygen concentration. In: Polarographic Oxygen
1251 Sensors. Aquatic and Physiological Applications. Gnaiger E, Forstner H (eds), Springer, Berlin,
1252 Heidelberg, New York:321-33.
- 1253 Garlid KD, Beavis AD, Ratkje SK (1989) On the nature of ion leaks in energy-transducing membranes.
1254 *Biochim Biophys Acta* 976:109-20.
- 1255 Garlid KD, Semrad C, Zinchenko V. Does redox slip contribute significantly to mitochondrial respiration? In:
1256 Schuster S, Rigoulet M, Ouhabi R, Mazat J-P, eds (1993) Modern trends in biothermokinetics. Plenum
1257 Press, New York, London:287-93.
- 1258 Gebert N, Joshi AS, Kutik S, Becker T, McKenzie M, Guan XL, Mooga VP, Stroud DA, Kulkarni G, Wenk MR,
1259 Rehling P, Meisinger C, Ryan MT, Wiedemann N, Greenberg ML, Pfanner N (2009) Mitochondrial
1260 cardiolipin involved in outer-membrane protein biogenesis: implications for Barth syndrome. *Curr Biol*
1261 19:2133-9.
- 1262 Gerö D, Szabo C (2016) Glucocorticoids suppress mitochondrial oxidant production via upregulation of
1263 uncoupling protein 2 in hyperglycemic endothelial cells. *PLoS One* 11:e0154813.
- 1264 Gibney E (2018) Largest overhaul of scientific units since 1875 wins approval. *Nature* 563:451-2.
1265 <https://www.nature.com/articles/d41586-018-07424-8>
- 1266 Gnaiger E (1993a). Efficiency and power strategies under hypoxia. Is low efficiency at high glycolytic ATP
1267 production a paradox? In: *Surviving Hypoxia: Mechanisms of Control and Adaptation*. Hochachka PW,
1268 Lutz PL, Sick T, Rosenthal M, Van den Thillart G, eds. CRC Press, Boca Raton, Ann Arbor, London,
1269 Tokyo:77-109.
- 1270 Gnaiger E (1993b) Nonequilibrium thermodynamics of energy transformations. *Pure Appl Chem* 65:1983-
1271 2002.
- 1272 Gnaiger E (2001) Bioenergetics at low oxygen: dependence of respiration and phosphorylation on oxygen
1273 and adenosine diphosphate supply. *Respir Physiol* 128:277-97.
- 1274 Gnaiger E (2009) Capacity of oxidative phosphorylation in human skeletal muscle. New perspectives of
1275 mitochondrial physiology. *Int J Biochem Cell Biol* 41:1837-45.
- 1276 Gnaiger E (2020) Mitochondrial pathways and respiratory control. An introduction to OXPHOS analysis. 5th
1277 ed. *Bioenerg Commun* 2020.2.
- 1278 Gnaiger E, Aasander Frostner E, Abdul Karim N, Abdel-Rahman EA, Abumrad NA, Acuna-Castroviejo D,
1279 Adiele RC, et al (2020) Mitochondrial respiratory states and rates. *Nat Metab* (in review)
- 1280 Gnaiger E, Méndez G, Hand SC (2000) High phosphorylation efficiency and depression of uncoupled
1281 respiration in mitochondria under hypoxia. *Proc Natl Acad Sci USA* 97:11080-5.
- 1282 Greggio C, Jha P, Kulkarni SS, Lagarrigue S, Broskey NT, Boutant M, Wang X, Conde Alonso S, Ofori E, Auwerx
1283 J, Cantó C, Amati F (2017) Enhanced respiratory chain supercomplex formation in response to exercise
1284 in human skeletal muscle. *Cell Metab* 25:301-11.
- 1285 Hinkle PC (2005) P/O ratios of mitochondrial oxidative phosphorylation. *Biochim Biophys Acta* 1706:1-11.
- 1286 Hofstadter DR (1979) Gödel, Escher, Bach: An eternal golden braid. A metaphorical fugue on minds and
1287 machines in the spirit of Lewis Carroll. Harvester Press:499 pp.
- 1288 Illaste A, Laasmaa M, Peterson P, Vendelin M (2012) Analysis of molecular movement reveals latticelike
1289 obstructions to diffusion in heart muscle cells. *Biophys J* 102:739-48.
- 1290 Jasienski M, Bazzaz FA (1999) The fallacy of ratios and the testability of models in biology. *Oikos* 84:321-
1291 26.
- 1292 Jepihhina N, Beraud N, Sepp M, Birkedal R, Vendelin M (2011) Permeabilized rat cardiomyocyte response
1293 demonstrates intracellular origin of diffusion obstacles. *Biophys J* 101:2112-21.
- 1294 Jezek P, Holendova B, Garlid KD, Jaburek M (2018) Mitochondrial uncoupling proteins: subtle regulators of
1295 cellular redox signaling. *Antioxid Redox Signal* 29:667-714.
- 1296 Karnkowska A, Vacek V, Zubáčová Z, Treitli SC, Petrželková R, Eme L, Novák L, Žárský V, Barlow LD, Herman
1297 EK, Soukal P, Hroudová M, Doležal P, Stairs CW, Roger AJ, Eliáš M, Dacks JB, Vlček Č, Hampl V (2016) A
1298 eukaryote without a mitochondrial organelle. *Curr Biol* 26:1274-84.
- 1299 Kenwood BM, Weaver JL, Bajwa A, Poon IK, Byrne FL, Murrow BA, Calderone JA, Huang L, Divakaruni AS,
1300 Tomsig JL, Okabe K, Lo RH, Cameron Coleman G, Columbus L, Yan Z, Saucerman JJ, Smith JS, Holmes JW,
1301 Lynch KR, Ravichandran KS, Uchiyama S, Santos WL, Rogers GW, Okusa MD, Bayliss DA, Hoehn KL (2013)
1302 Identification of a novel mitochondrial uncoupler that does not depolarize the plasma membrane. *Mol*
1303 *Metab* 3:114-23.
- 1304 Klepinin A, Ounpuu L, Guzun R, Chekulayev V, Timohhina N, Tepp K, Shevchuk I, Schlattner U, Kaambre T
1305 (2016) Simple oxygraphic analysis for the presence of adenylate kinase 1 and 2 in normal and tumor
1306 cells. *J Bioenerg Biomembr* 48:531-48.
- 1307 Koit A, Shevchuk I, Ounpuu L, Klepinin A, Chekulayev V, Timohhina N, Tepp K, Puurand M, Truu L, Heck K,
1308 Valvere V, Guzun R, Kaambre T (2017) Mitochondrial respiration in human colorectal and breast cancer
1309 clinical material is regulated differently. *Oxid Med Cell Longev* 1372640.

- 1310 Komlódi T, Tretter L (2017) Methylene blue stimulates substrate-level phosphorylation catalysed by
 1311 succinyl-CoA ligase in the citric acid cycle. *Neuropharmacology* 123:287-98.
- 1312 Korn E (1969) Cell membranes: structure and synthesis. *Annu Rev Biochem* 38:263-88.
- 1313 Lai N, M Kummitha C, Rosca MG, Fujioka H, Tandler B, Hoppel CL (2018) Isolation of mitochondrial
 1314 subpopulations from skeletal muscle: optimizing recovery and preserving integrity. *Acta Physiol*
 1315 (Oxf):e13182. doi: 10.1111/apha.13182.
- 1316 Lane N (2005) Power, sex, suicide: mitochondria and the meaning of life. Oxford University Press:354 pp.
- 1317 Larsen S, Nielsen J, Neigaard Nielsen C, Nielsen LB, Wibrand F, Stride N, Schroder HD, Boushel RC, Helge JW,
 1318 Dela F, Hey-Mogensen M (2012) Biomarkers of mitochondrial content in skeletal muscle of healthy
 1319 young human subjects. *J Physiol* 590:3349-60.
- 1320 Lee C, Zeng J, Drew BG, Sallam T, Martin-Montalvo A, Wan J, Kim SJ, Mehta H, Hevener AL, de Cabo R, Cohen
 1321 P (2015) The mitochondrial-derived peptide MOTS-c promotes metabolic homeostasis and reduces
 1322 obesity and insulin resistance. *Cell Metab* 21:443-54.
- 1323 Lee SR, Kim HK, Song IS, Youm J, Dizon LA, Jeong SH, Ko TH, Heo HJ, Ko KS, Rhee BD, Kim N, Han J (2013)
 1324 Glucocorticoids and their receptors: insights into specific roles in mitochondria. *Prog Biophys Mol Biol*
 1325 112:44-54.
- 1326 Leek BT, Mudaliar SR, Henry R, Mathieu-Costello O, Richardson RS (2001) Effect of acute exercise on citrate
 1327 synthase activity in untrained and trained human skeletal muscle. *Am J Physiol Regul Integr Comp*
 1328 *Physiol* 280:R441-7.
- 1329 Lemasters JJ, Nieminen AL, Qian T, Trost LC, Elmore SP, Nishimura Y, Crowe RA, Cascio WE, Bradham CA,
 1330 Brenner DA, Herman B (1998) The mitochondrial permeability transition in cell death: a common
 1331 mechanism in necrosis, apoptosis and autophagy. *Biochim Biophys Acta* 1366:177-96.
- 1332 Lemieux H, Blier PU, Gnaiger E (2017) Remodeling pathway control of mitochondrial respiratory capacity
 1333 by temperature in mouse heart: electron flow through the Q-junction in permeabilized fibers. *Sci Rep*
 1334 7:2840.
- 1335 Lemieux H, Semsroth S, Antretter H, Höfer D, Gnaiger E (2011) Mitochondrial respiratory control and early
 1336 defects of oxidative phosphorylation in the failing human heart. *Int J Biochem Cell Biol* 43:1729-38.
- 1337 Lenaz G, Tioli G, Falasca AI, Genova ML (2017) Respiratory supercomplexes in mitochondria. In:
 1338 Mechanisms of primary energy trasduction in biology. M Wikstrom (ed) Royal Society of Chemistry
 1339 Publishing, London, UK:296-337.
- 1340 Ling C, Rönn T (2019) Epigenetics in human obesity and type 2 diabetes. *Cell Metab* 29:1028-44.
 1341 <https://doi.org/10.1016/j.cmet.2019.03.009>.
- 1342 Liu S, Roellig DM, Guo Y, Li N, Frace MA, Tang K, Zhang L, Feng Y, Xiao L (2016) Evolution of mitosome
 1343 metabolism and invasion-related proteins in *Cryptosporidium*. *BMC Genomics* 17:1006.
- 1344 Lisowski P, Kannan P, Mlody B, Prigione A (2018) Mitochondria and the dynamic control of stem cell
 1345 homeostasis. *EMBO Rep* 19:e45432.
- 1346 Luo S, Valencia CA, Zhang J, Lee NC, Slone J, Gui B, Wang X, Li Z, Dell S, Brown J, Chen SM, Chien YH, Hwu WL,
 1347 Fan PC, Wong LJ, Atwal PS, Huang T (2018) Biparental inheritance of mitochondrial DNA in humans.
 1348 *Proc Natl Acad Sci U S A* doi: 10.1073/pnas.1810946115.
- 1349 Margulis L (1970) Origin of eukaryotic cells. New Haven: Yale University Press.
- 1350 McDonald AE, Vanlerberghe GC, Staples JF (2009) Alternative oxidase in animals: unique characteristics and
 1351 taxonomic distribution. *J Exp Biol* 212:2627-34.
- 1352 McKenzie M, Lazarou M, Thorburn DR, Ryan MT (2006) Mitochondrial respiratory chain supercomplexes
 1353 are destabilized in Barth Syndrome patients. *J Mol Biol* 361:462-9.
- 1354 Menshikova EV, Ritov VB, Fairfull L, Ferrell RE, Kelley DE, Goodpaster BH (2006) Effects of exercise on
 1355 mitochondrial content and function in aging human skeletal muscle. *J Gerontol A Biol Sci Med Sci* 61:534-
 1356 40.
- 1357 Menshikova EV, Ritov VB, Ferrell RE, Azuma K, Goodpaster BH, Kelley DE (2007) Characteristics of skeletal
 1358 muscle mitochondrial biogenesis induced by moderate-intensity exercise and weight loss in obesity. *J*
 1359 *Appl Physiol* (1985) 103:21-7.
- 1360 Menshikova EV, Ritov VB, Toledo FG, Ferrell RE, Goodpaster BH, Kelley DE (2005) Effects of weight loss and
 1361 physical activity on skeletal muscle mitochondrial function in obesity. *Am J Physiol Endocrinol Metab*
 1362 288:E818-25.
- 1363 Miller GA (1991) The science of words. Scientific American Library New York:276 pp.
- 1364 Mitchell P (1961) Coupling of phosphorylation to electron and hydrogen transfer by a chemi-osmotic type
 1365 of mechanism. *Nature* 191:144-8.
- 1366 Mitchell P (2011) Chemiosmotic coupling in oxidative and photosynthetic phosphorylation. *Biochim*
 1367 *Biophys Acta Bioenergetics* 1807:1507-38.
- 1368 MitoEAGLE Task Group (2020) Mitochondrial physiology. 1. Mitochondria and bioblasts. *Bioenerg Commun*
 1369 2020.#.

- 1370 MitoEAGLE Task Group (2020) Mitochondrial physiology. 3. Mitochondrial markers. *Bioenerg Commun*
1371 2020.#.
- 1372 Mogensen M, Sahlin K, Fernström M, Glintborg D, Vind BF, Beck-Nielsen H, Højlund K (2007) Mitochondrial
1373 respiration is decreased in skeletal muscle of patients with type 2 diabetes. *Diabetes* 56:1592-9.
- 1374 Mohr PJ, Phillips WD (2015) Dimensionless units in the SI. *Metrologia* 52:40-7.
- 1375 Moreno M, Giacco A, Di Munno C, Goglia F (2017) Direct and rapid effects of 3,5-diiodo-L-thyronine (T2).
1376 *Mol Cell Endocrinol* 7207:30092-8.
- 1377 Morrow RM, Picard M, Derbeneva O, Leipzig J, McManus MJ, Gouspillou G, Barbat-Artigas S, Dos Santos C,
1378 Hepple RT, Murdock DG, Wallace DC (2017) Mitochondrial energy deficiency leads to hyperproliferation
1379 of skeletal muscle mitochondria and enhanced insulin sensitivity. *Proc Natl Acad Sci U S A* 114:2705-10.
- 1380 Murley A, Nunnari J (2016) The emerging network of mitochondria-organelle contacts. *Mol Cell* 61:648-53.
- 1381 National Academies of Sciences, Engineering, and Medicine (2018) International coordination for science
1382 data infrastructure: Proceedings of a workshop—in brief. Washington, DC: The National Academies
1383 Press. doi: <https://doi.org/10.17226/25015>.
- 1384 Oemer G, Lackner L, Muigg K, Krumschnabel G, Watschinger K, Sailer S, Lindner H, Gnaiger E, Wortmann SB,
1385 Werner ER, Zschocke J, Keller MA (2018) The molecular structural diversity of mitochondrial
1386 cardiolipins. *Proc Nat Acad Sci U S A* 115:4158-63.
- 1387 Palmfeldt J, Bross P (2017) Proteomics of human mitochondria. *Mitochondrion* 33:2-14.
- 1388 Paradies G, Paradies V, De Benedictis V, Ruggiero FM, Petrosillo G (2014) Functional role of cardiolipin in
1389 mitochondrial bioenergetics. *Biochim Biophys Acta* 1837:408-17.
- 1390 Pesta D, Gnaiger E (2012) High-Resolution Respirometry. OXPHOS protocols for human cells and
1391 permeabilized fibres from small biopsies of human muscle. *Methods Mol Biol* 810:25-58.
- 1392 Pesta D, Hoppel F, Macek C, Messner H, Faulhaber M, Kobel C, Parson W, Burtscher M, Schocke M, Gnaiger E
1393 (2011) Similar qualitative and quantitative changes of mitochondrial respiration following strength and
1394 endurance training in normoxia and hypoxia in sedentary humans. *Am J Physiol Regul Integr Comp*
1395 *Physiol* 301:R1078-87.
- 1396 Price TM, Dai Q (2015) The role of a mitochondrial progesterone receptor (PR-M) in progesterone action.
1397 *Semin Reprod Med* 33:185-94.
- 1398 Puchowicz MA, Varnes ME, Cohen BH, Friedman NR, Kerr DS, Hoppel CL (2004) Oxidative phosphorylation
1399 analysis: assessing the integrated functional activity of human skeletal muscle mitochondria - case
1400 studies. *Mitochondrion* 4:377-85. Puntschart A, Claassen H, Jostarndt K, Hoppeler H, Billeter R (1995)
1401 mRNAs of enzymes involved in energy metabolism and mtDNA are increased in endurance-trained
1402 athletes. *Am J Physiol* 269:C619-25.
- 1403 Quiros PM, Mottis A, Auwerx J (2016) Mitonuclear communication in homeostasis and stress. *Nat Rev Mol*
1404 *Cell Biol* 17:213-26.
- 1405 Rackham O, Mercer TR, Filipovska A (2012) The human mitochondrial transcriptome and the RNA-binding
1406 proteins that regulate its expression. *WIREs RNA* 3:675-95.
- 1407 Rackham O, Shearwood AM, Mercer TR, Davies SM, Mattick JS, Filipovska A (2011) Long noncoding RNAs
1408 are generated from the mitochondrial genome and regulated by nuclear-encoded proteins. *RNA*
1409 17:2085-93.
- 1410 Reichmann H, Hoppeler H, Mathieu-Costello O, von Bergen F, Pette D (1985) Biochemical and
1411 ultrastructural changes of skeletal muscle mitochondria after chronic electrical stimulation in rabbits.
1412 *Pflugers Arch* 404:1-9.
- 1413 Renner K, Amberger A, Konwalinka G, Gnaiger E (2003) Changes of mitochondrial respiration,
1414 mitochondrial content and cell size after induction of apoptosis in leukemia cells. *Biochim Biophys Acta*
1415 1642:115-23.
- 1416 Rice DW, Alverson AJ, Richardson AO, Young GJ, Sanchez-Puerta MV, Munzinger J, Barry K, Boore JL, Zhang
1417 Y, dePamphilis CW, Knox EB, Palmer JD (2016) Horizontal transfer of entire genomes via mitochondrial
1418 fusion in the angiosperm *Amborella*. *Science* 342:1468-73.
- 1419 Rich P (2003) Chemiosmotic coupling: The cost of living. *Nature* 421:583.
- 1420 Rich PR (2013) Chemiosmotic theory. *Encyclopedia Biol Chem* 1:467-72.
- 1421 Roger JA, Munoz-Gomes SA, Kamikawa R (2017) The origin and diversification of mitochondria. *Curr Biol*
1422 27:R1177-92.
- 1423 Rostovtseva TK, Sheldon KL, Hassanzadeh E, Monge C, Saks V, Bezrukov SM, Sackett DL (2008) Tubulin
1424 binding blocks mitochondrial voltage-dependent anion channel and regulates respiration. *Proc Natl*
1425 *Acad Sci USA* 105:18746-51.
- 1426 Rustin P, Parfait B, Chretien D, Bourgeron T, Djouadi F, Bastin J, Rötig A, Munnich A (1996) Fluxes of
1427 nicotinamide adenine dinucleotides through mitochondrial membranes in human cultured cells. *J Biol*
1428 *Chem* 271:14785-90.

- 1429 Saks VA, Veksler VI, Kuznetsov AV, Kay L, Sikk P, Tiivel T, Tranqui L, Olivares J, Winkler K, Wiedemann F,
1430 Kunz WS (1998) Permeabilised cell and skinned fiber techniques in studies of mitochondrial function in
1431 vivo. *Mol Cell Biochem* 184:81-100.
- 1432 Salabei JK, Gibb AA, Hill BG (2014) Comprehensive measurement of respiratory activity in permeabilized
1433 cells using extracellular flux analysis. *Nat Protoc* 9:421-38.
- 1434 Sazanov LA (2015) A giant molecular proton pump: structure and mechanism of respiratory complex I. *Nat*
1435 *Rev Mol Cell Biol* 16:375-88.
- 1436 Schneider TD (2006) Claude Shannon: biologist. The founder of information theory used biology to
1437 formulate the channel capacity. *IEEE Eng Med Biol Mag* 25:30-3.
- 1438 Schönfeld P, Dymkowska D, Wojtczak L (2009) Acyl-CoA-induced generation of reactive oxygen species in
1439 mitochondrial preparations is due to the presence of peroxisomes. *Free Radic Biol Med* 47:503-9.
- 1440 Schultz J, Wiesner RJ (2000) Proliferation of mitochondria in chronically stimulated rabbit skeletal muscle-
1441 -transcription of mitochondrial genes and copy number of mitochondrial DNA. *J Bioenerg Biomembr*
1442 32:627-34.
- 1443 Simson P, Jepihhina N, Laasmaa M, Peterson P, Birkedal R, Vendelin M (2016) Restricted ADP movement in
1444 cardiomyocytes: Cytosolic diffusion obstacles are complemented with a small number of open
1445 mitochondrial voltage-dependent anion channels. *J Mol Cell Cardiol* 97:197-203.
- 1446 Singh BK, Sinha RA, Tripathi M, Mendoza A, Ohba K, Sy JAC, Xie SY, Zhou J, Ho JP, Chang CY, Wu Y, Giguère V,
1447 Bay BH, Vanacker JM, Ghosh S, Gauthier K, Hollenberg AN, McDonnell DP, Yen PM (2018) Thyroid
1448 hormone receptor and ERR α coordinately regulate mitochondrial fission, mitophagy, biogenesis, and
1449 function. *Sci Signal* 11(536) DOI: 10.1126/scisignal.aam5855.
- 1450 Speijer D (2016) Being right on Q: shaping eukaryotic evolution. *Biochem J* 473:4103-27.
- 1451 Stucki JW, Ineichen EA (1974) Energy dissipation by calcium recycling and the efficiency of calcium
1452 transport in rat-liver mitochondria. *Eur J Biochem* 48:365-75.
- 1453 Sugiura A, Mattie S, Prudent J, McBride HM (2017) Newly born peroxisomes are a hybrid of mitochondrial
1454 and ER-derived pre-peroxisomes. *Nature* 542:251-4.
- 1455 Tonkonogi M, Harris B, Sahlin K (1997) Increased activity of citrate synthase in human skeletal muscle after
1456 a single bout of prolonged exercise. *Acta Physiol Scand* 161:435-6.
- 1457 Torralba D, Baixauli F, Sánchez-Madrid F (2016) Mitochondria know no boundaries: mechanisms and
1458 functions of intercellular mitochondrial transfer. *Front Cell Dev Biol* 4:107. eCollection 2016.
- 1459 Vamecq J, Schepers L, Parmentier G, Mannaerts GP (1987) Inhibition of peroxisomal fatty acyl-CoA oxidase
1460 by antimycin A. *Biochem J* 248:603-7.
- 1461 Waczulikova I, Habodaszova D, Cagalinec M, Ferko M, Ulicna O, Mateasik A, Sikurova L, Ziegelhöffer A (2007)
1462 Mitochondrial membrane fluidity, potential, and calcium transients in the myocardium from acute
1463 diabetic rats. *Can J Physiol Pharmacol* 85:372-81.
- 1464 Wagner BA, Venkataraman S, Buettner GR (2011) The rate of oxygen utilization by cells. *Free Radic Biol*
1465 *Med* 51:700-712.
- 1466 Wang H, Hiatt WR, Barstow TJ, Brass EP (1999) Relationships between muscle mitochondrial DNA content,
1467 mitochondrial enzyme activity and oxidative capacity in man: alterations with disease. *Eur J Appl Physiol*
1468 *Occup Physiol* 80:22-7.
- 1469 Watt IN, Montgomery MG, Runswick MJ, Leslie AG, Walker JE (2010) Bioenergetic cost of making an
1470 adenosine triphosphate molecule in animal mitochondria. *Proc Natl Acad Sci U S A* 107:16823-7.
- 1471 Weibel ER, Hoppeler H (2005) Exercise-induced maximal metabolic rate scales with muscle aerobic
1472 capacity. *J Exp Biol* 208:1635-44.
- 1473 White DJ, Wolff JN, Pierson M, Gemell NJ (2008) Revealing the hidden complexities of mtDNA inheritance.
1474 *Mol Ecol* 17:4925-42.
- 1475 Wikström M, Hummer G (2012) Stoichiometry of proton translocation by respiratory complex I and its
1476 mechanistic implications. *Proc Natl Acad Sci U S A* 109:4431-6.
- 1477 Williams EG, Wu Y, Jha P, Dubuis S, Blattmann P, Argmann CA, Houten SM, Amariuta T, Wolski W, Zamboni
1478 N, Aebersold R, Auwerx J (2016) Systems proteomics of liver mitochondria function. *Science* 352
1479 (6291):aad0189
- 1480 Willis WT, Jackman MR, Messer JL, Kuzmiak-Glancy S, Glancy B (2016) A simple hydraulic analog model of
1481 oxidative phosphorylation. *Med Sci Sports Exerc* 48:990-1000.
- 1482 Yoshinaga MY, Kellermann MY, Valentine DL, Valentine RC (2016) Phospholipids and glycolipids mediate
1483 proton containment and circulation along the surface of energy-transducing membranes. *Prog Lipid Res*
1484 64:1-15.
- 1485 Zíková A, Hampl V, Paris Z, Týč J, Lukeš J (2016) Aerobic mitochondria of parasitic protists: diverse genomes
1486 and complex functions. *Mol Biochem Parasitol* 209:46-57.
- 1487
- 1488

1489 ***Authors (MitoEAGLE Task Group): for list of authors and affiliations, see:**
 1490 https://www.bioenergetics-communications.org/index.php/BEC2020.1_doi10.26124bec2020-0001.v1
 1491

1492 **Author contributions:** This manuscript developed as an open invitation to scientists and students to join
 1493 as coauthors in the bottom-up spirit of COST, based on a first draft written by the corresponding author,
 1494 who integrated coauthor contributions in a sequence of Open Access versions. Coauthors contributed to the
 1495 scope and quality of the manuscript, may have focused on a particular section, and are listed in alphabetical
 1496 order. Coauthors confirm that they have read the final manuscript and agree to implement the
 1497 recommendations into future manuscripts, presentations and teaching materials.
 1498

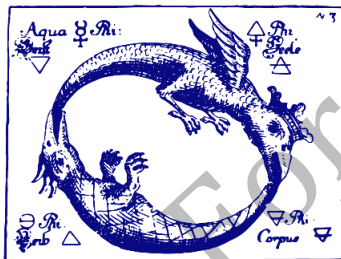


COST Action CA15203 MitoEAGLE

1499 **Acknowledgements:** We thank Marija Beno for management assistance, and Peter R Rich for valuable
 1500 discussions. This publication is based upon work from COST Action MitoEAGLE, supported by COST
 1501 (European Cooperation in Science and Technology), in cooperation with COST Actions CA16225 EU-
 1502 CARDIOPROTECTION and CA17129 CardioRNA; K-Regio project MitoFit funded by the Tyrolian
 1503 Government, and project NextGen-02k which has received funding from the European Union's Horizon
 1504 2020 research and innovation programme under grant agreement No. 859770.
 1505

1506 **Competing financial interests:** Erich Gnaiger is founder and CEO of Oroboros Instruments, Innsbruck,
 1507 Austria.
 1508

1509 **Corresponding author:** Erich Gnaiger
 1510 Chair COST Action CA15203 MitoEAGLE – <http://www.mitoeagle.org>
 1511 Department of Visceral, Transplant and Thoracic Surgery, D. Swarovski Research Laboratory, Medical
 1512 University of Innsbruck, Innrain 66/4, A-6020 Innsbruck, Austria
 1513 Email: mitoeagle@i-med.ac.at; Tel: +43 512 566796, Fax: +43 512 566796 20
 1514



BIOENERGETICS COMMUNICATIONS

1515 **Copyright:** © 2020 The authors. This is an Open Access communication distributed under the terms of the
 1516 Creative Commons Attribution License, which permits unrestricted use, distribution, and reproduction in
 1517 any medium, provided the original authors and source are credited. © remains with the authors, who have
 1518 granted Bioenergetics Communications an Open Access publication licence in perpetuity.